PTCH. Even though the GLI proteins may well not be the only mediators of Shh signaling, the overwhelming majority of available data on insects and vertebrates indicates a central role for GLI proteins in regulating the mediation and interpretation of Shh signals. As shown in Fig. 3, the expression of all three *PTCH* isoforms was elevated by GLI1 in the cell lines we employed. However, a closer observation revealed slight differences in the degree of induction. For example, *PTCHd* and *PTCHb* were more strongly upregulated by GLI1 in 293T and HSC-2 cells, whereas the induction of *PTCHa* was more evident than that of *PTCHb* or *PTCHd* in Ho-1-u-1 and LK-2 cells, indicating cell type-specific regulation of the isoforms.

PTCH promoter has functional GLI-binding sites

The *Drosophila patched* gene (*ptc*) has a cluster of three GLI consensus binding sites (5′-TGGGTGGTC-3′ or 5′-GACCACCCA-3′) [21] in the promoter region that is required for the reporter gene expression in response to Hedgehog (Hh) activity [22]. Recently, it was reported that the transcriptional regulation of *PTCH* by Shh signaling was mediated by a single GLI-binding site located ~400 bp upstream of exon 1b (GLI-BS1 in Fig. 4A) [23]. However, sequencing farther upstream indicated the presence of even two more consensus GLI-binding sequences not reported previously (GLI-BS2 and GLI-BS3 in Fig. 4A, −3965 and −8283 bp relative to the reported transcription start site of exon 1b, respectively). The mouse upstream sequence also contained three putative consensus GLI-binding sites and

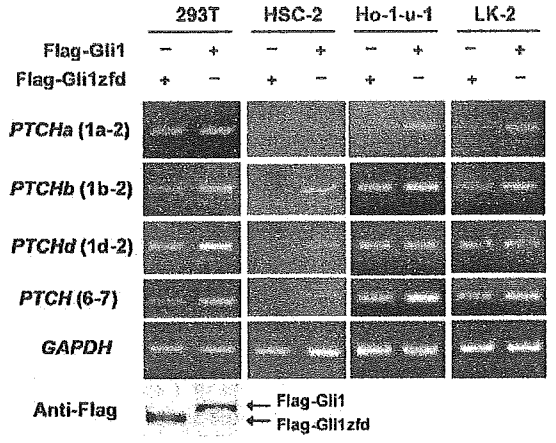

Fig. 3. Transcriptional regulation of three *PTCH* isoforms. Cell lines indicated at the top were transfected with the expression plasmid pSRα-Flag-Gli1 or pSRα-Flag-Gli1zfd. pSRα-Flag-Gli1zfd is a plasmid for a mutant GLI1 lacking the zinc finger domain [43] used as a negative control for pSRα-Flag-Gli1. Cells were cultured in 0.5% FCS for 16 h after the transfection and total RNA was extracted from the transfected cells and subjected to RT-PCR. Forward and reverse primers were constructed for the exons indicated in parentheses. PTCH (6–7) indicates the overall *PTCH* expression because exons 6 and 7 are used regardless of the isoform. The expression of Flag-tagged GLI1 proteins was confirmed by immunoblotting using anti-Flag antibody (Anti-Flag).

the sequences around these sites were strikingly conserved (Fig. 4B). This suggests that two upstream consensus GLI-binding sequences, as well as a reported one, act as GLI-responsive elements. To test this assumption, genome fragments containing GLI-BS1, GLI-BS2, and GLI-BS3 were inserted into a luciferase construct (pGV-PTCH1, pGV-PTCH2, and pGV-PTCH3, respectively). Cotransfection of the GLI1 expression plasmid with pGV-PTCH1 enhanced the luciferase activity in SH-SY5Y cells (Fig. 4C), confirming a previous report. In addition, as anticipated, GLI1 expression also enhanced the luciferase activity when cotransfected with reporter constructs containing upstream GLI-binding sequences (pGV-PTCH2 and pGV-PTCH3). To confirm that these sites are really responsible for the GLI-mediated activation, a mutation with four nucleotide substitutions was introduced into GLI-binding sequences (5′-T*A*GT*GG*A*C*TC-3′ or 5′-GA*TCCACTA*-3′, mutated nucleotides in italic), generating the constructs pGV-PTCH1mt, pGV-PTCH2mt, and pGV-PTCH3mt. The introduction of these mutations into the putative GLI-binding sites indeed abolished the elevation of luciferase activity induced by GLI1. Furthermore, the 1.1-kb mouse fragment containing GLI-BS1 showed a similar response to GLI1 expression (pGV-mPTCH) (Fig. 4C), suggesting that the mechanism by which *PTCH* expression is regulated by the Shh signaling pathway is conserved.

We also examined whether GLI protein could physically associate with putative GLI-binding elements in *PTCH* in vitro and in vivo. First, we tested these sites in an electrophoretic mobility shift assay. As shown in Fig. 4D, when GST–GLI3 fusion protein was incubated with a wild-type DNA probe containing a putative GLI consensus sequence in the promoter region, a complex with a shift in gel mobility was detected (lane 3). In contrast, substitution of GST nonfusion for GST–GLI3, or mutant DNA probe with the same nucleotide substitutions as described above for the wild-type sequence, resulted in a failure to detect a complex whose mobility was altered in these assays (lanes 2 and 6). Moreover, the DNA–protein complex was abolished by competition with an unlabeled oligonucleotide containing the GLI site, but not by a mutated oligonucleotide, demonstrating the specificity of the complex formation (lanes 4 and 5). GST–GLI3 also bound specifically to two more upstream sequences with a GLI-binding consensus sequence (lanes 9 and 15) in vitro.

To determine whether the GLI protein occupies these sites in vivo, we used a chromatin immunoprecipitation (ChIP) assay to analyze lysates extracted from 293T cells transfected with a plasmid to express Flag–GLI1. The genomic fragments including GLI-BS1 and GLI-BS3 were specifically precipitated as a GLI–DNA complex with an anti-Flag antibody (Fig. 4E, lanes 3 and 11), while GLI-BS2 was barely coimmunoprecipitated (lane 7). As controls, the same fragments were not precipitated when cells were transfected with a construct for Flag tag or the lysates were incubated with an anti-Myc antibody (lanes 2, 4, 10, and

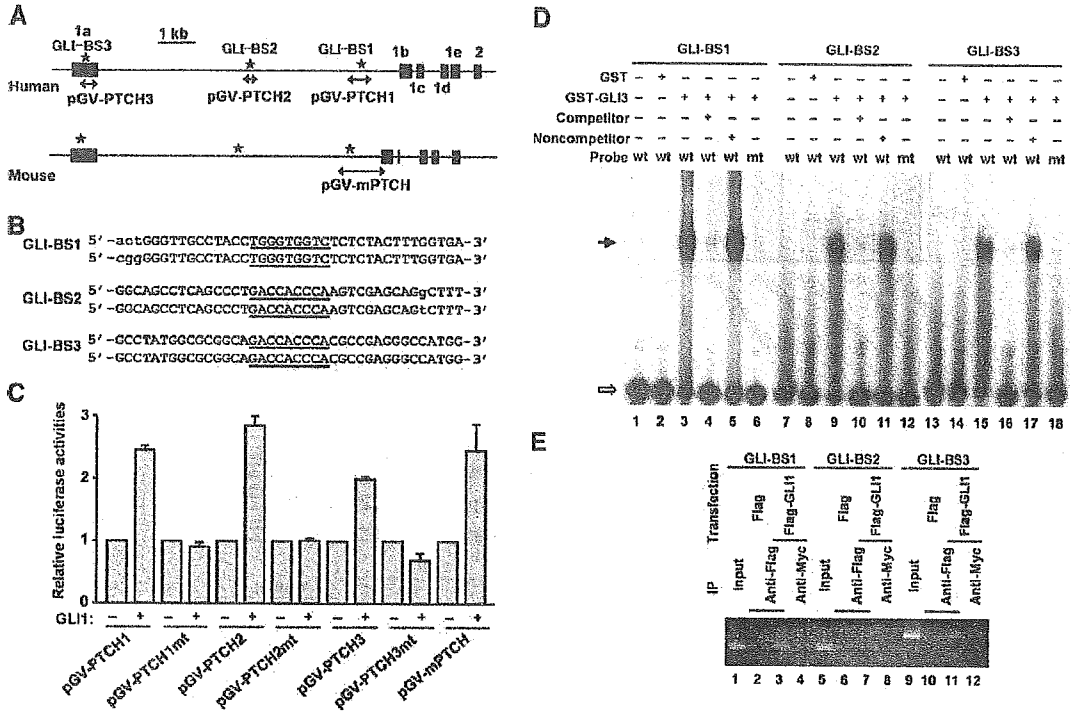

Fig. 4. Transcriptional regulation of *PTCH* isoforms. (A) Comparison of human and mouse genomic structures. Black boxes indicate locations and relative sizes of exons. Asterisks indicate the positions of three putative GLI-binding sequences (5′-TGGGTGGTC-3′ or 5′-GACCACCCA-3′). DNA fragments inserted into luciferase vectors to make the reporter gene constructs are indicated by arrows. The names of the resulting constructs are indicated below. (B) Comparison of human (top) and mouse (bottom) GLI-binding sequences. Consensus GLI-binding sequences are underlined. Lowercase letters indicate nucleotides not conserved between the two species. (C) The *PTCH* promoter is GLI responsive. SH-SY5Y cells were cotransfected with various reporter gene constructs as indicated with or without pSRα-Flag-GLI1. Cells were cultured in 0.5% FCS for 16 h after the transfection and then harvested for the luciferase assay. Firefly luciferase activity was normalized by *Renilla* luciferase activity from a cotransfected pRL-SV40 and is indicated relative to the activity of the same reporter without pSRα-Flag-GLI1. The total amount of transfected DNA was adjusted using pcDNA3.0. Data are representative of three experiments with similar results. (D) GLI protein can bind in vitro to an oligonucleotide probe representing the *PTCH* gene region. Recombinant GST or GST–GLI3 protein was incubated with ^{32}P-labeled oligonucleotide DNA probes containing a putative GLI-consensus sequence (wt) or a mutated version with four nucleotide substitutions (mt), together with or without a 50-fold molar excess of cold competitor containing the GLI site (competitor) or its mutant (noncompetitor). DNA–protein complexes were size fractionated in a nondenaturing polyacrylamide gel and were detected by autoradiography. The positions of the free probe and the shifted complexes are indicated by the open and closed arrows, respectively. (E) Identification of GLI-binding region in vivo. ChIP assay was performed with genomic fragments including the putative GLI-binding consensus sequence indicated at the top. Chromatin from 293T cells transfected with pCI-Flag (lanes 2, 6, 10) or pFlag-GLI1 (lanes 3, 4, 7, 8, 11, 12) was immunoprecipitated with anti-Flag antibody (lanes 2, 3, 6, 7, 10, 11). PCR amplification was performed with corresponding templates. Input represents a portion of the sonicated chromatin before immunoprecipitation. Anti-Myc antibody was used as a negative control (lanes 4, 8, 12).

12). Taken together, our data show that at least GLI-BS1 and GLI-BS3 are involved in GLI-mediated *PTCH* expression. In contrast, GLI-BS2 is not accessible to GLI in vivo, probably due to a higher genomic structure, although the accessibility may be cell-type dependent.

Functional analysis of three isoforms of PTCH

In 293T cells, overexpression of PTCH protein causes apoptosis and inhibition of cell proliferation [24,25]. Thus, it is expected that there is a basal level of leakage activity of Smo that excess PTCH prevents in the apparent absence of Shh. The fact that cyclopamine has a proapoptotic effect in these cells supports this possibility (discussed below). On the basis of this background, we performed a functional analysis of the PTCH isoforms using a GLI-responsive luciferase reporter in 293T cells. Luciferase activities were suppressed when 293T cells were transfected with plasmids for $PTCH_L$ and $PTCH_M$ but not with an empty vector, pcDNA3.0 (Fig. 5A). This suppression was not observed when cells were transfected with the plasmid for *PTCHΔC* which encodes only 194 N-terminal amino acid residues, indicating the specificity of the results. To investigate the function of PTCH in vivo, PTCH was transiently expressed in 293T cells. As expected, $PTCH_L$ and $PTCH_M$ induced apoptosis in 293T cells as measured by assessing the sub-G0/G1 population (Fig. 5B). However, they were not as potent as cyclopamine, a well-known inhibitor of Shh signaling [26]. This is probably, at least in part, due to the presence of untransfected cells. Interestingly, in contrast to $PTCH_L$ and $PTCH_M$, $PTCH_S$ did not significantly suppress GLI-responsive luciferase activity or induce apoptosis, implying that this isoform does not have the expected function of a PTCH protein or the expression level of this isoform

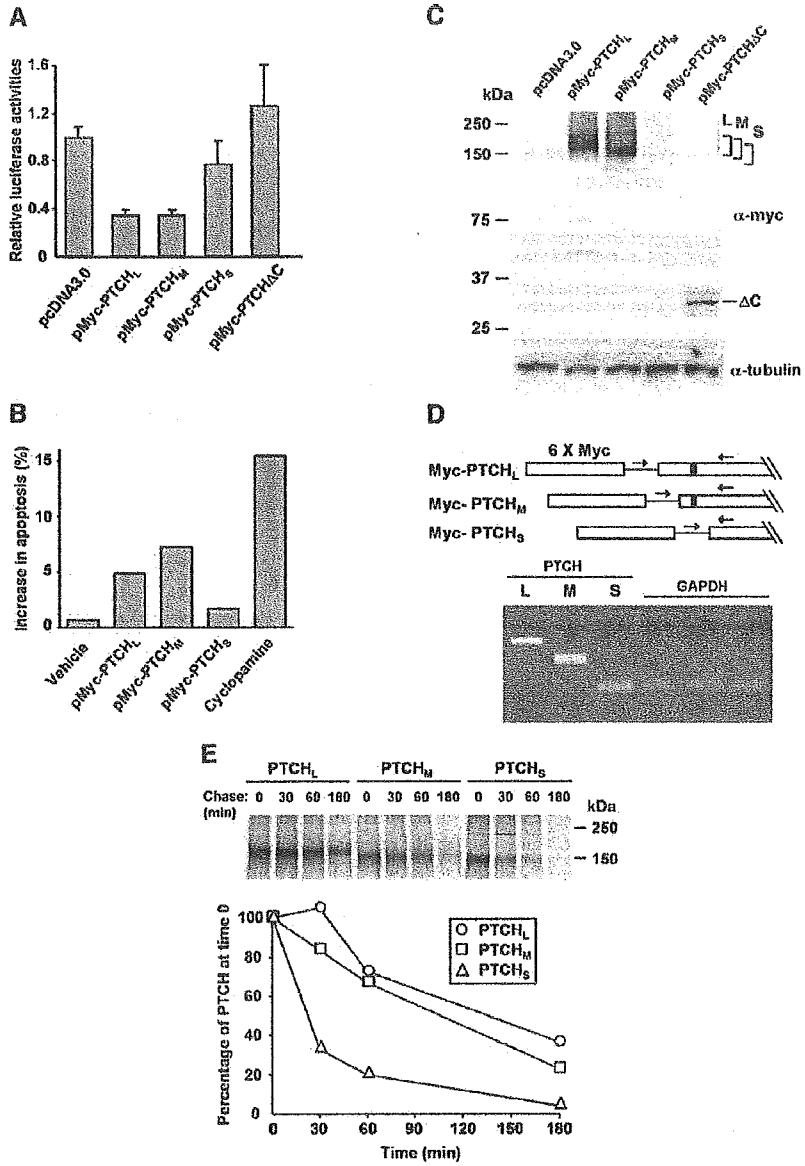

Fig. 5. Functional analysis of PTCH isoforms. (A) Inhibition of GLI-responsive luciferase activity by PTCH. 293T cells were transfected with various expression plasmids as indicated together with 8 × GLI-Luc containing eight GLI-binding sites and LTR-LacZ. After the transfection, cells were cultured in 0.5% FCS for 16 h and then harvested for the luciferase assay. Firefly luciferase activity was normalized to β-galactosidase activity from a cotransfected LTR-lacZ vector. Data are representative of three experiments with similar results. (B) PTCH-induced cell death as measured based on DNA content. 293T cells were transfected with plasmids for PTCH or treated with cyclopamine or vehicle alone (ethanol). The induction of apoptosis was assessed by the increase in the subG0/G1 population compared with mock-transfected cells. (C) Protein levels of expressed genes. Cell lysates were obtained from 293T cells transfected with indicated plasmids and subjected to immunoblotting with an anti-c-Myc antibody. Tubulin is a loading control. The molecular weights of the four PTCH protein products predicted from the composition of amino acid residues, including the Myc tag, are as follows: $PTCH_L$, 172 kDa; $PTCH_M$, 163 kDa; $PTCH_S$, 154 kDa; PTCHΔC, 32.2 kDa. (D) RT-PCR analysis of expressed genes. Total RNA was extracted from 293T cells transfected with plasmids for each isoform of *PTCH* and RT-PCR analysis was performed using primers depicted at the top. A forward primer was constructed in the linker region between the Myc tag and *PTCH* and a reverse primer in exon 2. Filled boxes indicate the position of the first transmembrane domain. GAPDH is an internal control for RT-PCR. (E) Metabolic labeling of the PTCH proteins. 293T cells transfected with a construct for PTCH were pulse-labeled with [^{35}S]methionine and chased for the indicated periods. ^{35}S-labeled PTCH was immunoprecipitated, detected by autoradiography (top), and then quantified by phosphorimaging. Levels of labeled PTCH are plotted relative to the amount present at time 0 (bottom).

is too low to cause these changes. To examine these possibilities, we first investigated the protein levels of each PTCH isoform by immunoblotting. Compared with $PTCH_L$, $PTCH_M$, and PTCHΔC, the protein level of $PTCH_S$ was markedly reduced (Fig. 5C). The diffuse migration of PTCH proteins is thought to be due to glycosylation as reported [27,28]. However, when RT-PCR was performed to analyze mRNA levels, these three isoforms were found to be expressed at comparable levels (Fig. 5D). These results indicate that the stability of $PTCH_S$ protein is compromised.

To determine whether the reduced activity of $PTCH_S$ was due to decreased protein stability, we measured the half-life of the three isoforms. 293T cells transfected with a plasmid for each isoform were metabolically labeled with [^{35}S]-methionine and then incubated with excess unlabeled amino acids for various lengths of time. PTCH proteins were immunoprecipitated and size-separated by SDS–PAGE. As shown in Fig. 5E, Myc-tagged PTCH proteins were visualized at a point corresponding to approximately the same size as that detected by immunoblotting. Following a 180-min chase, 36 and 23% of de novo synthesized $PTCH_L$ and $PTCH_M$, respectively, remained in 293T cells. Half-lives were calculated as 115 and 83 min, respectively. In contrast, the degradation of $PTCH_S$ was considerably accelerated, such that 5% of the protein remained at 180 min (half-life 26 min). These results indicated that $PTCH_S$ is an unstable protein compared with $PTCH_L$ and $PTCH_M$.

Discussion

Alternative pre-mRNA splicing is an important mechanism for generating protein diversity and may explain in part how mammalian complexity arises from a surprisingly small complement of genes. It also plays important roles in development and disease. A recent study estimated that greater than 55% of human genes are alternatively spliced [29] and that about 10% of the mutations in the human genome affect the canonical splice site sequence [30]. In particular, isoforms of genes with alternative first exons may have distinct mechanisms of expression. For example, the *DSCR1* (Down syndrome candidate region 1)/*MCIP1* (modulatory calcineurin-interacting protein 1) and *nNOS* (neuronal nitric oxide synthase) genes have four and eight alternative first exons, respectively, and are subjected to a distinct expressional regulation by separate promoters [31,32].

In this study, we identified and characterized five alternative first exons in both human and mouse *PTCH* genes encoding four protein species. Thus, arguably, *PTCH* is one of the most complex human genes in terms of diversity at the 5′ end. The transcription of all major isoforms was upregulated by GLI1, an upstream transcription factor in the Shh pathway, although the degree of activation was cell type-specific. Unlike *Drosophila ptc* in which only a single transcript has been reported and whose promoter has a cluster of three GLI-binding consensus sequences in a 130-bp region [22], human and mouse *PTCH* have three consensus sequences dispersed over 7.5 kb between exon 1a and exon 1b (Fig. 4A). Since exons 1b, 1c, 1d, and 1e are located close to each other, it is likely that *PTCH* isoforms except *PTCHa* are regulated by at least partially overlapping promoters, including GLI-BS1 in Fig. 4A. In contrast, exon 1a is located ~8 kb upstream of exon 1b and one of the GLI-binding sites is located inside exon 1a and the other two are located far downstream. No GLI-binding consensus sequence was found in the promoter region of *PTCHa* (i.e., upstream of exon 1a), at least not up to the 40 kb position. Thus, taking our results with the ChIP assay into consideration, it is likely that the two GLI-binding sequences, one in exon 1a and the other far downstream of exon 1a (GLI-BS3 and GLI-BS1 in Fig. 4A, respectively), are responsible for the GLI-mediated regulation of *PTCHa*. This is not unexpected because *hepatocyte nuclear factor-3β*, another target gene of Shh signaling, has a GLI-binding site 3′ of the transcription unit and this site is essential for the response to Shh [33]. Although NBCCS families who show linkage to chromosomal regions other than 9q22.3–q31, to where *PTCH* has been mapped, have not been reported, a considerable number of NBCCS patients do not have mutations within the coding region of *PTCH* [34–36]. Therefore, taking our results into account, it is warranted to examine mutations in GLI-binding sequences using samples from such patients. Interestingly, *PTCH2*, another homologue of the *Drosophila Hh* gene, whose mutations are found in BCC and medulloblastoma [37], also has a GLI-binding consensus sequence ~470 bp upstream of the first methionine codon (based on the genomic sequence, AL136380), indicating that *PTCH2* is another target gene of the Shh pathway. Supporting this notion, PTCH2 is upregulated in basal cell carcinoma in which Shh signaling is activated [38].

$PTCH_L$ and $PTCH_M$ were equally potent in terms of suppressing GLI-mediated transcription or inducing apoptosis. In contrast, the $PTCH_S$ protein was less potent due to its instability. Amino acid residues 101–119 of $PTCH_L$ and 35–53 of $PTCH_M$ comprise the first transmembrane domain, which is absent in $PTCH_S$ because it starts with Met^{152} in $PTCH_L$ (Fig. 1D). This probably explains why $PTCH_S$ is unstable. However, $PTCH_S$ was more ubiquitously expressed throughout adult tissues than the other two, implying that, despite its instability, $PTCH_S$ may be important for tissue homeostasis or tumor suppression. It is possible that a certain extracellular stress or stimulus such as the binding of Shh may stabilize $PTCH_S$. In contrast, the expression of $PTCH_L$ was always predominant during embryonic development, indicating that $PTCH_L$ plays a key role in embryogenesis.

The generation of mice in which one of the isoforms is nonfunctional may help clarify the roles of the alternative proteins in normal development and carcinogenesis. In this study, we focused on the usage of alternative first exons. However, some cell-surface receptors, such as CD44, undergo a complex, combinatorial splicing that determines the function of the gene products [39]. Although the major transcripts of human and mouse *PTCH* are ~8 kb long [18,20], we have identified rare transcripts lacking exons 4 and 5 (K.N. and T.M., unpublished data). Therefore, a comprehensive study of alternative pre-mRNA splicing throughout the gene using cost-effective and high-throughput methods, such as polymerase colony technology [40] or

exon junction microarrays [41], may shed light on the functional complexity of the *PTCH* gene and carcinogenesis with increased Shh pathway activity.

Materials and methods

Isolation of human PTCH isoforms and construction of plasmids

To obtain 5′ ends of cDNA, RNA ligase-mediated 5′RACE was performed using the GeneRacer kit (Invitrogen) according to the manufacturer's directions. Random primers were used to reverse transcribe RNA. A reverse gene-specific primer was constructed in exon 2 to amplify the first-strand cDNA. The amplified cDNA was subcloned into pCR4-TOPO (Invitrogen) and sequenced. The expression plasmid encoding Myc-tagged $PTCH_L$ (pMyc-Ptc1) was kindly provided by Dr. Jeffrey Ming. To make expression plasmids for $PTCH_M$ and $PTCH_S$, a DNA fragment encoding the N-terminal region of $PTCH_L$ was excised from pMyc-Ptc1 by digestion with *Eco*RI and replaced with the RT-PCR product encoding the N-terminal region of $PTCH_M$ or $PTCH_S$, respectively. To make luciferase constructs, pGV-PTCH1, pGV-PTCH2, and pGV-PTCH3, fragments for the human *PTCH* promoter ranging from bp −1354 to −746, −4105 to −3808, and −8427 to −8032, respectively, relative to the reported transcription start site (GenBank Accession No. NM_000264) were subcloned into pGV-P2 (Wako Chemicals, Osaka, Japan). Mutated plasmids for these constructs were created by PCR-mediated mutagenesis as described previously [42]. The authenticity of all constructs was confirmed by DNA sequencing. The expression vector for FLAG-GLI1, pSRα-Flag-GLI1 [43], and the reporter vector, 8 × GLI-Luc [33], were kindly provided by Dr. Alexander L. Joyner and Hiroshi Sasaki, respectively.

Cell culture and transfections

The human embryonic kidney cell line 293T and mouse embryonal carcinoma cell line P19 were maintained in DMEM supplemented with 10% fetal calf serum (FCS), 50 U/ml penicillin, and 0.1 mg/ml streptomycin at 37°C in a humidified atmosphere of 5% CO_2. The human neuroblastoma line SH-SY5Y, oral squamous cell carcinoma lines HSC-2 and Ho-1-u-1, and lung squamous cell carcinoma line LK-2 (obtained from Cell Resource Center for Biomedical Research, Tohoku University, Japan) were maintained similarly except that RPMI 1640 medium was used. Cells were transfected with the indicated plasmids using Effectene reagent (Qiagen) and harvested at 16 h after the lipofection.

Analysis of PTCH isoform expression profiles

Human and mouse *PTCH* cDNA was amplified by RT-PCR using 0.5 μg of total RNA purified from a panel of human tissues (Ambion and Clontech) or mouse embryos and primers 5′-CTGGGAGAAGACGGAGGA-GC-3′ (exon 1a forward, human), 5′-CCCGGGAAATTA-ATAAAAGG-3′ (exon 1a forward, mouse), 5′-GGACCG-GGACTATCTGCACC-3′ (exon 1b forward, human), 5′-GGACCGGGACTATCTGCACC-3′ (exon 1b forward, mouse), 5′-CCTCTCCAGGAAAAGCAGCA-3′ (exon 1c forward, human), 5′-GAGAAAGCAGCAGACAAGT-GAAGGTTG-3′ (exon 1c forward, mouse), 5′-ATCC-ATGTGGCTGCCCTCTT-3′ (exon 1d forward, human), 5′-ATCCTTGTGGCCGCCCTCTT-3′ (exon 1d forward, mouse), 5′-TTCTCGGCGGG-GGTCCAGTT-3′ (exon 1e forward, human), 5′-CCAGA-TGGACCACGGTTGCTG-TAGATT-3′ (exon 1e forward, mouse), 5′-CACAGCTC-CTCCACGTTGGT-3′ (exon 2 reverse, human), and 5′-CA-CAGCTCCTCCACGTTGGT-3′ (exon 2 reverse, mouse). During the log phase of amplification (25–35 cycles depending on the templates), 1 μl of the PCR product was applied onto a DNA LabChip (Agilent Technologies) and loaded into an Agilent 2100 bioanalyzer according to the manufacturer's protocol. Data analysis was performed with Agilent 2100 bioanalyzer software. The expression of *PTCH* was normalized to that of the glyceraldehyde-3-phosphate dehydrogenas (*GAPDH*) gene or β-actin gene.

Western blotting

Immunoblot analysis was performed as described previously [44]. In brief, 30 μg of the cell lysate was subjected to SDS–PAGE and transferred onto a nitrocellulose membrane. The membrane was incubated with anti-c-Myc (Santa Cruz, 9E10) or anti-Flag (Sigma, M2) mouse monoclonal antibody followed by horseradish peroxidase-conjugated anti-mouse immunoglobulins (DAKO). The proteins were visualized using enhanced chemiluminescence immunoblotting detection reagents (Amersham).

Luciferase assay

293T or SH-SY5Y cells growing on six-well culture plates were cotransfected using Effectene reagent with various combinations of plasmids as indicated in the figure legends. Transfected cells were maintained in 0.5% FCS for 16 h and then harvested for the luciferase assay using the reagents and protocols provided by Promega or Wako chemicals.

Electrophoretic mobility shift assay

To obtain GST–GLI3 fusion protein, *Escherichia coli* strain BL21(DE3)pLysS (Novagen) was transformed with pGST-GLI3MF [45] (a gift from Dr. Shunsuke Ishii), which encodes the metal finger region of GLI3. The fusion protein was purified by affinity chromatography using glutathione–Sepharose 4B (Amersham Pharmacia Biotech) according to the manufacturer's instructions. The ^{32}P-labeled double-stranded oligonucleotide probes containing the sequence

for a consensus GLI-binding site (5′-TTGCCTACCTG-GGTGGTCTCTCTACTT-3′, 5′-CTCAGCCCTGA-CCACCCAAGTCGAGCA-3′, and 5′-GGCGCGGCAG-ACCACCCACGCCGAGGG-3′) or a mutated sequence (5′-TTGCCTACCT*AGTGGA*TCTCTCTACTT-3′, 5′-CT-CAGCCCTGA*TCCACT*AAGTCGAGCA-3′, and 5′-GG-CGCGGCAGA*TCCACT*ACGCCGAGGG-3′) (mutated nucleotides in italic) were incubated with the GST or GST–GLI3 fusion (200 ng). The reaction was performed in 10 μl of binding buffer containing 4% glycerol, 1 mM $MgCl_2$, 0.5 mM EDTA, 50 mM NaCl, 10 mM Tris–HCl (pH 7.5), and 0.05 mg/ml poly(dI–dC) for 20 min at room temperature. For competition experiments, a 50-fold molar excess of unlabeled, double-stranded oligonucleotide, containing either a GLI site or a mutated GLI site as described above, was included in binding reactions. Samples were fractionated on a nondenaturing 6% polyacrylamide gel and visualized by autoradiography.

Apoptosis assay

293T cells were plated at 4×10^5 per well onto a six-well plate, grown for 16 h, transfected with plasmids for Myc-tagged PTCH or treated with cyclopamine (Toronto Research Chemicals, Inc.) (5 μM final concentration), and then grown in DMEM with 0.5% FCS. After 24 h, relative DNA content was determined by flow cytometry as described previously [46]. Cells having a reduced DNA content (sub-G0/G1) were regarded as apoptotic.

Pulse–chase experiment

293 cells were plated at 8×10^5 cells per 60-mm plate, cultured for 24 h, and transfected with 1 μg of PTCH expression plasmid using the Lipofectamine Plus reagent kit (Invitrogen) according to the manufacturer's instructions. Twenty-four hours after the transfection, cells were incubated with DMEM lacking methionine (−Met) for 30 min and then with 16.7 μCi/ml of L-[^{35}S]methionine with DMEM − Met for 2 h. Cells were washed three times with phosphate-buffered saline (PBS) and incubated with DMEM supplemented with 2 mM methionine for varying periods. At each time point, cells were scraped, washed with PBS, and lysed in 300 μl of lysis buffer containing 150 mM NaCl, 1% Triton X-100, 10 mM Tris–HCl (pH 7.4), 5 mM EDTA, 1 mM PMSF, 18 μg/ml aprotinin, 50 μg/ml leupeptin, 1 mM benzamidine, and 0.7 μg/ml pepstatin. The extracts were pelleted at 16,000*g* for 15 min at 4°C, and the supernatants (200 μl) were immunoprecipitated for 16 h with 20 μl of protein–A/G agarose (Santa Cruz) and 3 μl of anti-c-Myc antibody. The immunoprecipitates were washed three times with 1 ml of lysis buffer, solubilized in 20 μl of 1 × Laemmli buffer by heating at 95°C for 5 min, and resolved on a 5–20% gradient polyacrylamide gel. Gels were dried, exposed, and analyzed using a FUJIX BAS2000 imaging analyzer (Fuji Film).

ChIP assay

ChIP assay was performed using the acetyl-histone H3 ChIP Assay Kit (Upstate Biotechnology), as recommended by the manufacturer, except that monoclonal anti-Flag (M2) and anti-Myc antibodies (9E10) were used in this study. 293T cells were plated at 1×10^6 cells per 10-cm dish, grown for 16 h, and then transfected with pFlag-Gli1 or pCI-Flag (encoding Flag-tag epitope). After 24 h, genomic DNA and protein were cross-linked by addition of formaldehyde (1% final concentration) directly to the culture medium and incubated for 10 min at 37°C. Cells were lysed in 1 ml of SDS lysis buffer containing 1% SDS, 10 mM EDTA, and 50 mM Tris–HCl (pH 8.1) and sonicated to generate 300- to 1000-bp DNA fragments. After centrifugation, the cleared supernatant was diluted 10-fold with ChIP dilution buffer and incubated with the specific antibody at 4°C for 16 h with rotation before incubation with protein A–Sepharose beads at 4°C for 1 h with rotation. Immune complexes were precipitated, washed, and eluted as recommended. DNA–protein cross-links were reversed by heating to 65°C for 2.5 h. DNA was phenol extracted, ethanol precipitated, and resuspended in 20 μl of Tris–EDTA. We used 2.5 μl of each sample as a template for PCR. PCR amplification was performed using primers that flank the putative GLI-response elements, 5′-AAAGGC-TGGAGCTCCCGCCC-3′ (GLI-BS1, forward) and 5′-T-GCGCGCAAAGGCATCCCAC-3′ (GLI-BS1, reverse), or 5′-GGGCATGCATATTAAAGCCG-3′ (GLI-BS2, forward) and 5′-CGAGCGCTATCTTAATCTCC-3′ (GLI-BS2, reverse), or 5′-AGCGCCTGTTTACCCAGGAG-3′ (GLI-BS3, forward) and 5′-GCTCCTCCGTCTTCTCCCAG-3′ (GLI-BS3, reverse).

Acknowledgments

We thank Mayu Yamazaki for technical support, Kayoko Saito for preparing the manuscript, and Drs. J. Ming (Children's Hospital of Philadelphia), A. Joyner (NYU Medical Center), S. Ishii (Tsukuba Life Science Center, RIKEN), and H. Sasaki (Center for Developmental Biology, RIKEN) for providing plasmids. This work was supported by Grants for Brain Research, Cancer Research, Genome Research, and Child Health and Development from the Ministry of Health, Labor, and Welfare, and a Grant-in-Aid for Scientific Research and the Budget for Nuclear Research from the Ministry of Education, Culture, Sports, Science, and Technology of Japan.

References

[1] E. Belloni, et al., Identification of *Sonic hedgehog* as a candidate gene responsible for holoprosencephaly, Nat. Genet. 14 (1996) 353–356.
[2] E. Roessler, et al., Mutations in the human *Sonic hedgehog* gene cause holoprosencephaly, Nat. Genet. 14 (1996) 357–360.

[3] C. Chiang, et al., Cyclopia and defective axial patterning in mice lacking *Sonic hedgehog* gene function, Nature 383 (1996) 407–431.
[4] H. Hahn, et al., Mutations of the human homolog of Drosophila *patched* in the nevoid basal cell carcinoma syndrome, Cell 85 (1996) 841–851.
[5] R.L. Johnson, et al., Human homolog of *patched*, a candidate gene for the basal cell nevus syndrome, Science 272 (1996) 1668–1671.
[6] A.B. Unden, et al., Mutations in the human homologue of *Drosophila patched* (*PTCH*) in basal cell carcinomas and the Gorlin syndrome: different *in vivo* mechanisms of PTCH inactivation, Cancer Res. 56 (1996) 4562–4565.
[7] C. Raffel, et al., Sporadic medulloblastomas contain *PTCH* mutations, Cancer Res. 57 (1997) 842–845.
[8] T. Pietsch, et al., Medulloblastomas of the desmoplastic variant carry mutations of the human homologue of Drosophila patched, Cancer Res. 57 (1997) 2085–2088.
[9] R.J. Gorlin, Nevoid basal-cell carcinoma syndrome, Medicine 66 (1987) 98–113.
[10] M.R. Gailani, et al., The role of the human homologue of *Drosophila patched* in sporadic basal cell carcinomas, Nat. Genet. 14 (1996) 78–81.
[11] J. Xie, et al., Activating Smoothened mutations in sporadic basal-cell carcinoma, Nature 391 (1998) 90–92.
[12] S.P. Thayer, et al., Hedgehog is an early and late mediator of pancreatic cancer tumorigenesis, Nature 425 (2003) 851–856.
[13] D.M. Berman, et al., Widespread requirement for Hedgehog ligand stimulation in growth of digestive tract tumours, Nature 425 (2003) 846–851.
[14] D.N. Watkins, et al., Hedgehog signalling within airway epithelial progenitors and in small-cell lung cancer, Nature 422 (2003) 313–317.
[15] P.W. Ingham, A.P. McMahon, Hedgehog signaling in animal development: paradigms and principles, Genes Dev. 15 (2001) 3059–3087.
[16] D.M. Berman, Medulloblastoma growth inhibition by hedgehog pathway blockade, Science 297 (2002) 1559–1561.
[17] P. Kogerman, et al., Alternative first exons of *PTCH1* are differentially regulated *in vivo* and may confer different functions to the PTCH1 protein, Oncogene 21 (2002) 6007–6016.
[18] L.V. Goodrich, R.L. Johnson, L. Milenkovic, J.A. McMahon, M.P. Scott, Conservation of the hedgehog/patched signaling pathway from flies to mice: induction of a mouse patched gene by Hedgehog, Genes Dev. 10 (1996) 301–312.
[19] Q. Wu, A.R. Krainer, AT-AC pre-mRNA splicing mechanisms and conservation of minor introns in voltage-gated ion channel genes, Mol. Cell Biol. 19 (1999) 3225–3236.
[20] H. Hahn, et al., A mammalian *patched* homolog is expressed in target tissues of *sonic hedgehog* and maps to a region associated with developmental abnormalities, J. Biol. Chem. 271 (1996) 12125–12128.
[21] K.W. Kinzler, B. Vogelstein, The GLI gene encodes a nuclear protein which binds specific sequences in the human genome, Mol. Cell Biol. 10 (1990) 634–642.
[22] C. Alexandre, A. Jacinto, P.W. Ingham, Transcriptional activation of *hedgehog* target genes in *Drosophila* is mediated directly by the cubitus interruptus protein, a member of the GLI family of zinc finger DNA-binding proteins, Genes Dev. 10 (1996) 2003–2013.
[23] M. Ågren, P. Kogerman, M.I. Kleman, M. Wessling, R. Toftgård, Expression of the *PTCH1* tumor suppressor gene is regulated by alternative promoters and a single functional Gli-binding site, Gene 330 (2004) 101–114.
[24] E.A. Barnes, M. Kong, V. Ollendorff, D.J. Donoghue, Patched1 interacts with cyclin B1 to regulate cell cycle progression, EMBO J. 20 (2001) 2214–2223.
[25] C. Thibert, et al., Inhibition of neuroepithelial patched-induced apoptosis by sonic hedgehog, Science 301 (2003) 843–846.
[26] J.K. Chen, J. Taipale, M.K. Cooper, P.A. Beachy, Inhibition of Hedgehog signaling by direct binding of cyclopamine to Smoothened, Genes Dev. 16 (2002) 2743–2748.
[27] E.C. Bailey, L. Milenkovic, M.P. Scott, J.F. Collawn, R.L. Johnson, Several *PATCHED1* missense mutations display activity in *patched1*-deficient fibroblasts, J. Biol. Chem. 277 (2002) 33632–33640.
[28] V. Marigo, R.A. Davey, Y. Zuo, J.M. Cunningham, C.J. Tabin, Biochemical evidence that patched is the Hedgehog receptor, Nature 384 (1996) 176–179.
[29] Z. Kan, E.C. Rouchka, W.R. Gish, D.J. States, Gene structure prediction and alternative splicing analysis using genomically aligned ESTs, Genome Res. 11 (2001) 889–900.
[30] P.D. Stenson, et al., Human Gene Mutation Database (HGMD): 2003 update, Hum. Mutat. 21 (2003) 577–581.
[31] J.J. Fuentes, M.A. Pritchard, X. Estivill, Genomic organization, alternative splicing, and expression patterns of the *DSCR1* (Down syndrome candidate region 1) gene, Genomics 44 (1997) 358–361.
[32] Y. Wang, et al., RNA diversity has profound effects on the translation of neuronal nitric oxide synthase, Proc. Natl. Acad. Sci. U.S.A. 96 (1999) 12150–12155.
[33] H. Sasaki, C. Hui, M. Nakafuku, H. Kondoh, A binding site for Gli proteins is essential for *HNF-3β* floor plate enhancer activity in transgenics and can respond to Shh in vitro, Development 124 (1997) 1313–1322.
[34] K. Fujii, et al., Mutations in the human homologue of *Drosophila patched* in Japanese nevoid basal cell carcinoma syndrome patients, Hum. Mutat. 21 (2003) 451–452.
[35] A. Chidambaram, et al., Mutations in the human homologue of the Drosophila *patched* gene in Caucasian and African-American nevoid basal cell carcinoma syndrome patients, Cancer Res. 56 (1996) 4599–4601.
[36] C. Wicking, et al., Most germ-line mutations in the nevoid basal cell carcinoma syndrome lead to a premature termination of the PATCHED protein, and no genotype–phenotype correlations are evident, Am. J. Hum. Genet. 60 (1997) 21–26.
[37] I. Smyth, et al., Isolation and characterization of human *patched 2* (*PTCH2*), a putative tumour suppressor gene in basal cell carcinoma and medulloblastoma on chromosome 1p32, Hum. Mol. Genet. 8 (1999) 291–297.
[38] P.G. Zaphiropoulos, A.B. Undén, F. Rahnama, R.E. Hollingsworth, R. Toftgård, *PTCH2*, a novel human patched gene, undergoing alternative splicing and up-regulated in basal cell carcinomas, Cancer Res. 59 (1999) 787–792.
[39] J. Lesley, R. Hyan, CD44 structure and function, Front. Biosci. 3 (1998) D616–D630.
[40] J. Zhu, J. Shendure, R.D. Mitra, G.M. Church, Single molecule profiling of alternative pre-mRNA splicing, Science 301 (2003) 836–838.
[41] J.M. Johnson, et al., Genome-wide survey of human alternative pre-mRNA splicing with exon junction microarrays, Science 302 (2003) 2141–2144.
[42] Y. Imai, Y. Matsushima, T. Sugimura, M. Terada, A simple and rapid method for generating a deletion by PCR, Nucleic Acids Res. 19 (1991) 2785.
[43] H.L. Park, et al., Mouse *Gli1* mutants are viable but have defects in SHH signaling in combination with a *Gli2* mutation, Development 127 (2000) 1593–1605.
[44] T. Miyashita, Y. Okamura-Oho, Y. Mito, S. Nagafuchi, M. Yamada, Dentatorubral pallidoluysian atrophy (DRPLA) protein is cleaved by caspase-3 during apoptosis, J. Biol. Chem. 272 (1997) 29238–29242.
[45] P. Dai, et al., Sonic Hedgehog-induced activation of the *Gli1* promoter is mediated by GLI3, J. Biol. Chem. 274 (1999) 8143–8152.
[46] K. Fujii, et al., γ-Irradiation deregulates cell cycle control and apoptosis in nevoid basal cell carcinoma syndrome-derived cells, Jpn. J. Cancer Res. 90 (1999) 1351–1357.
[47] B.C. Schaefer, Revolutions in rapid amplification of cDNA ends: new strategies for polymerase chain reaction cloning of full-length cDNA ends, Anal. Biochem. 227 (1995) 255–273.

European Journal of Neuroscience, Vol. 22, pp. 3036–3046, 2005

Chondroitinase ABC combined with neural stem/progenitor cell transplantation enhances graft cell migration and outgrowth of growth-associated protein-43-positive fibers after rat spinal cord injury

Takeshi Ikegami,[1,2] Masaya Nakamura,[1] Junichi Yamane,[1,2,3] Hiroyuki Katoh,[1] Seiji Okada,[2,3] Akio Iwanami,[1,2,3] Kota Watanabe,[1,3] Ken Ishii,[1] Fumikazu Kato,[4] Hiroshi Fujita,[5] Toyomi Takahashi,[4] Hirotaka James Okano,[2,3] Yoshiaki Toyama[1] and Hideyuki Okano[2,3]

[1]Department of Orthopaedic Surgery, Keio University School of Medicine, Tokyo, Japan
[2]Department of Physiology, Keio University School of Medicine, 35 Shinanomachi, Shinjuku, Tokyo, 160-8582, Japan
[3]Core Research for Evolutional Science and Technology, Japan Science and Technology Agency, Saitama, Japan
[4]Central Research Laboratories, Seikagaku Corporation, Tokyo, Japan
[5]Glycoconjugate Research Center, Seikagaku Corporation, Kanagawa, Japan

Keywords: central nervous system repair, chondroitin sulfate proteoglycan, glial scar, growth-associated protein-43, neural stem cell

Abstract

We previously reported that the transplantation of neural stem/progenitor cells (NSPCs) can contribute to the repair of injured spinal cord in adult rats and monkeys. In some cases, however, most of the transplanted cells adhered to the cavity wall and failed to migrate and integrate into the host spinal cord. In this study we focused on chondroitin sulfate proteoglycan (CSPG), a known constituent of glial scars that is strongly expressed after spinal cord injury (SCI), as a putative inhibitor of NSPC migration *in vivo*. We hypothesized that the digestion of CSPG by chondroitinase ABC (C-ABC) might promote the migration of transplanted cells and neurite outgrowth after SCI. An *in vitro* study revealed that the migration of NSPC-derived cells was inhibited by CSPG and that this inhibitory effect was attenuated by C-ABC pre-treatment. Consistently, an *in vivo* study of C-ABC treatment combined with NSPC transplantation into injured spinal cord revealed that C-ABC pre-treatment promoted the migration of the transplanted cells, whereas CSPG-immunopositive scar tissue around the lesion cavity prevented their migration into the host spinal cord in the absence of C-ABC pre-treatment. Furthermore, this combined treatment significantly induced the outgrowth of a greater number of growth-associated protein-43-positive fibers at the lesion epicentre, compared with NSPC transplantation alone. These findings suggested that the application of C-ABC enhanced the benefits of NSPC transplantation for SCI by reducing the inhibitory effects of the glial scar, indicating that this combined treatment may be a promising strategy for the regeneration of injured spinal cord.

Introduction

With the aim of regenerating injured spinal cord, various types of intraspinal cellular transplants have been investigated in many laboratories. We have previously shown that the transplantation of neural stem/progenitor cells (NSPCs) into injured spinal cord contributes to the repair of injured spinal cord in adult rats (Ogawa *et al.*, 2002; Okano *et al.*, 2003; Watanabe *et al.*, 2004) and non-human primates (Iwanami *et al.*, 2005). However, in some cases, most of the transplanted cells adhered to the cavity wall and did not migrate and integrate with the host spinal cord. Insufficient integration between the transplanted cells and the host spinal cord might result in a limited anatomic and functional recovery after spinal cord injury (SCI) (Predy & Malhotra, 1989; Grijalva *et al.*, 1996). The formation of scarring tissue after contusion injury might obstruct an adequate integration between transplant and host, thereby blocking the potentially beneficial effect of the transplantation on functional recovery (Das, 1983; Nornes *et al.*, 1983; Houle & Reier, 1988; Reier *et al.*, 1988). Recent studies have shown that chondroitin sulfate proteoglycan (CSPG) is one of the inhibitory molecules found in glial scars after SCI (Fitch & Silver, 1997; Monnier *et al.*, 2003; Tang *et al.*, 2003) and that the digestion of CSPG by chondroitinase ABC (C-ABC) promotes axonal regeneration and functional recovery (Lemons *et al.*, 1999; Bradbury *et al.*, 2002; Jones *et al.*, 2002; Yick *et al.*, 2003). We hypothesized that CSPG deposition diminished the beneficial effects of NSPC transplantation for the treatment of SCI by inhibiting the migration and integration of the transplanted cells into the host spinal cord and that the digestion of CSPG might provide a more favorable environment for the kinetics of transplanted NSPCs, resulting in improved regeneration of the injured spinal cord. In this study, we investigated the inhibitory effect of CSPG on NSPCs with respect to their migration, viability and differentiation and examined whether C-ABC attenuates this effect *in vitro*. Furthermore, we applied C-ABC intrathecally in combination with NSPC transplantation to examine the synergistic effects of this combined treatment on injured spinal cord.

Correspondence: Dr Hideyuki Okano, [2]Department of Physiology, as above.
E-mail: hidokano@sc.itc.keio.ac.jp

Received 24 May 2005, revised 2 September 2005, accepted 10 October 2005

doi:10.1111/j.1460-9568.2005.04492.x

Materials and methods

All surgical interventions and animal care procedures were in accordance with the Laboratory Animal Welfare Act, the Guide for the Care and Use of Laboratory Animals (National Institute of Health, USA) and the Guidelines and Policies for Animal Surgery provided by the Animal Study Committee of the Central Institute for Experimental Animals of Keio University and were approved by the ethics committee of Keio University.

Preparation of neural stem/progenitor cells

We previously demonstrated that *in vitro* expanded NSPCs could differentiate into mature neurons, astrocytes and oligodendrocytes after transplantation into the injured spinal cord (Ogawa *et al.*, 2002; Watanabe *et al.*, 2004). NSPCs were cultured and expanded as neurospheres according to the method described previously (Reynolds & Weiss, 1992; Reynolds *et al.*, 1992; Ogawa *et al.*, 2002; Watanabe *et al.*, 2004). NSPCs were cultured and expanded as described previously (Reynolds *et al.*, 1992; Reynolds & Weiss, 1992; Watanabe *et al.*, 2004). Briefly, using a sterile technique, the striata of Sprague-Dawley rats were dissected out on embryonic day 14, from a pregnant rat deeply anesthetized with ether. The striatal tissue was suspended in culture medium and dissociated by mechanical trituration with a fire-polished glass Pasteur pipette. The cells were then collected by centrifugation and resuspended in a hormone-rich and serum-free culture medium containing recombinant human epidermal growth factor (20 ng/mL; Pepro Tech, Rocky Hill, NJ, USA) and recombinant human fibroblast growth factor-2 (20 ng/mL; Pepro Tech). Passage was performed once every 4–5 days and NSPCs after the third passage were used throughout the entire assay.

Migration assay

The well bottoms of a sterile 48-well plate were directly coated first with poly-L-lysine (25 μg/mL; Sigma) and then with one of the following three coatings: laminin (20 μg/mL; Sigma), CSPG (5 μg/mL; CC117, Chemicon) plus laminin (20 μg/mL) or CSPG (5 μg/mL) plus laminin (20 μg/mL) followed by treatment with C-ABC (3.3 U/mL; Seikagaku, Tokyo, Japan) for 2 h at 37 °C. (N.B. Throughout this report, wells coated with laminin alone are denoted 'laminin-coated wells', those coated with CSPG plus laminin are denoted 'CSPG-coated wells' and those treated with C-ABC after CSPG plus laminin coating are denoted 'C-ABC-treated wells'.) Cells were plated in each well (40 neurospheres/cm^2) and incubated at 37 °C in culture medium without epidermal growth factor or fibroblast growth factor-2. After 12 h of incubation, the cells were fixed with 4% paraformaldehyde for 10 min. Three samples were evaluated under each set of conditions and 10 neurospheres were randomly captured at 100× magnification under an inverted microscope (Eclipse TS100, Nikon, Tokyo, Japan) equipped with a CCD camera (DP70, Olympus, Tokyo, Japan). The migration distance was calculated as the mean of the straight-line measurement from the edge of the neurosphere to the farthest defined edge of the migratory cell boundary in four vertical directions (Kearns *et al.*, 2003) using an MCID system (Imaging Research, Toronto, Ontario, Canada). Thereafter, the cells were incubated overnight at 4 °C with the anti-nestin antibody (mouse monoclonal, 1 : 200; Chemicon) and then with appropriate secondary antibodies (Alexa Fluor 568 anti-mouse IgG, 1 : 1000; Molecular Probes, Eugene, OR, USA) and Hoechst 33258 (Sigma) at room temperature (23 °C) for 1 h. The samples were captured under a fluorescent microscope (Eclipse TS100) equipped with a CCD camera (DP70).

Survival assay

Lentivirally transduced NSPCs expressing intense luciferase protein were previously developed by Okada *et al.* (2005). These genetically modified neurospheres were plated on laminin- or CSPG-coated wells at a density of 40 neurospheres/cm^2. The cells were then incubated at 37 °C in culture medium without epidermal growth factor or fibroblast growth factor-2. Twelve hours later, luciferin (150 μg/mL; Xenogen, Alameda, CA, USA) was added to each well, the cells were incubated for 10 min and the photon count of each well was measured using a Xenogen IVIS 100 System (SC BioScience, Tokyo, Japan). The photon count is directly proportional to cell viability, as the release of photons by living cells relies on an adenosine triphosphate- and oxygen-dependent photochemical reaction between luciferin and luciferase (Sweeney *et al.*, 1999; Contag & Bachmann, 2002; Shah *et al.*, 2003). Nine samples were evaluated under each set of conditions.

Differentiation assay

To examine the effect of CSPG on the differentiation of NSPCs *in vitro*, a differentiation assay was performed as described previously (Watanabe *et al.*, 2004). In brief, neurospheres derived from green rats ubiquitously expressing enhanced green fluorescent protein (Ito *et al.*, 2001) were dissociated into single cells and plated into laminin- or CSPG-coated wells (6×10^4 cells/cm^2). The cells were incubated at 37 °C in culture medium without epidermal growth factor or fibroblast growth factor-2. Four days after plating, the cells were fixed with 4% paraformaldehyde and immunostained with the following primary antibodies: anti-green fluorescent protein (GFP) antibody (rabbit polyclonal, 1 : 500; MBL, Woburn, MA, USA) and anti-neuronal class III β-tubulin antibody (TuJ1, mouse monoclonal, 1 : 500; BAbCO, Richmond, CA, USA) for neurons, anti-GFP antibody (mouse monoclonal, 1 : 500; Molecular Probes) and anti-glial fibrillary acidic protein antibody (rabbit polyclonal, 1 : 500; Dako, Glostrup, Denmark) for astrocytes and anti-GFP antibody (rabbit polyclonal, 1 : 500; MBL) and anti-2′3′-cyclic nucleotide 3′-phosphodiesterase antibody (mouse monoclonal, 1 : 500; Sigma) for oligodendrocytes. The cells were incubated with appropriate secondary antibodies (Alexa Fluor 568, 488 anti-rabbit IgG, 1 : 1000; 568, 488 anti-mouse IgG, 1 : 1000; Molecular Probes) and counterstained with Hoechst 33258. Four samples were evaluated under each set of conditions and five fields were randomly captured at 200× magnification under a fluorescent microscope (Eclipse TS100) equipped with a CCD camera (DP70). The nuclei were counted after Hoechst staining and the numbers of TuJ1-, glial fibrillary acidic protein- and 2′3′-cyclic nucleotide 3′-phosphodiesterase-immunopositive cells, all of which were positive for GFP, in each field were quantified. The numbers were summed to obtain a representative total count for each sample and the percentages of each phenotype were calculated.

Spinal cord injury

Adult (230–250 g) female Sprague-Dawley rats (Clea Japan) were used for all the experimental groups. All surgeries were performed under intraperitoneal anesthesia with chloral hydrate (0.35 mg/g body weight). Spinal contusion lesions were made using a standardized device (NYU impactor) developed for the Multicentre Animal Spinal Cord Injury Study (MASCIS) (Gruner, 1992). Briefly, a laminectomy

was performed at the Th10 level and the exposed dura was then contused by a 10-g weight dropped from a height of 25 mm. The rats were returned to their cages with free access to water and food. Manual bladder expression was performed twice per day until reflex bladder emptying was re-established. The reliability of the NYU impactor used in the present study can be monitored and the monitoring allowed impacts that did not achieve expected values to be legitimately discarded according to the previous report of Gruner (1992).

Chondroitin sulfate proteoglycan expression after spinal cord injury

To determine the appropriate period for applying C-ABC to injured spinal cord *in vivo*, we investigated the time course of CSPG expression after SCI using immunohistochemistry. The rats were killed at 4 days, 2, 4 and 8 weeks after injury under deep ether anesthesia. Spinal cord tissue was removed at each time point, processed into sagittal frozen sections and immunostained with CS56 antibody as described in the Immunohistochemistry section.

Activity measurement of chondroitinase ABC solution

Sterile lyophilized C-ABC was dissolved in physiological saline at a concentration of 200 U/mL. An enzyme aliquot was kept at 37 °C in the presence of polymeric beads (Alzeid chemical compatibility test kit, Durect, Cupertino, CA, USA) consisting of the same materials as the Alzet osmotic pump reservoir. Enzyme activity was measured based on the increase in A_{232} using a method described by Yamagata *et al.* (1968). Enzyme aliquots sampled at defined intervals were incubated again with chondroitin-6-sulfate, sodium acetate and Tris-HCl, pH 8.0. After incubation at 37 °C for 20 min, the reaction was stopped by heating for 1 min in a boiling water bath. The reaction mixture was then diluted with 10 volumes of 50 mM HCl and the u.v. absorption of the resultant solution was measured at 232 nm against the blank mixture. One unit of enzyme was defined as the amount required to eliminate cleavage of the substrate, yielding u.v.-absorbing materials corresponding to 1 μmol of Δ^4-hexuronate residues per min, as calculated with a value of 5500 for its molar absorption coefficient. All trials were carried out in quadruplicate.

Continuous intrathecal infusion of chondroitinase ABC

To prepare for infusion, an enzyme aliquot (200 U/mL, 0.2 mL) was loaded into the reservoir of an Alzet 2001 osmotic pump (Durect) and incubated overnight in normal saline at 37 °C before tube insertion. As a control, C-ABC solution (200 U/mL) inactivated at 60 °C for 24 h was used. At 1 week after SCI, the rats were anesthetized again and a partial laminectomy was performed at the T13 level. A small incision was made in the lateral meninges and a silicon tube (outer diameter 0.7 mm; Imamura, Tokyo, Japan) attached to the osmotic pump was advanced slowly into the subarachnoid space. The tip of the silicon tube was placed just caudal to the level of injury (vertebral T11). The rats in the C-ABC group ($n = 26$) and the inactivated C-ABC group ($n = 23$) received infusions through loaded osmotic pumps for 1 week. After 1 week of infusion, a subset of the rats was killed for the immunohistochemistry study (C-ABC group, $n = 3$; inactivated C-ABC group, $n = 2$) and the high-performance liquid chromatography (HPLC) assay (C-ABC group, $n = 9$; inactivated C-ABC group, $n = 9$). The rats killed for the immunohistochemistry study were perfused with 4% paraformaldehyde, processed and immunostained with CS56 or 2B6 antibody, as described in the Immunohistochemistry section. The injured spinal cords of the rats killed for the HPLC assay were removed and processed as described in the HPLC assay section. The other rats (C-ABC group, $n = 14$; inactivated C-ABC group, $n = 12$) were used for NSPC transplantation.

Transplantation of neural stem/progenitor cells into injured spinal cord

After 1 week of infusion (i.e. 2 weeks after SCI), neurospheres derived from the striatum of green rats were transplanted into the injured spinal cord of C-ABC-infused ($n = 14$) and inactivated C-ABC-infused ($n = 7$) rats. For NSPC transplantation, a glass micropipette attached to a Hamilton syringe was inserted into the spinal cord and 5 μL of the neurosphere suspension (2×10^8 cells/mL) was injected using a stereotaxic injector (KDS 310, Muromachi-kikai, Tokyo, Japan) at a rate of 1 μL/min into the epicentre of the injured spinal cord. Culture medium alone was injected into the other rats in the inactivated C-ABC-infused group (vehicle control group, $n = 5$). Six weeks after the NSPC transplantation, the rats were killed for immunohistochemistry.

High-performance liquid chromatography assay

The rats infused with C-ABC ($n = 9$) or inactivated C-ABC ($n = 9$) from 1 to 2 weeks after SCI were killed at the end of the infusion period under deep ether anesthesia. Naive animals ($n = 4$) were used as controls. The 10-mm length of injured spinal cord tissue was removed and immediately frozen in liquid nitrogen and stored at −80 °C until use. Glycosaminoglycans in the spinal cord were analysed using a previously reported method (Shinmei *et al.*, 1992). The specimen was digested with actinase E and the digest was then centrifuged. The supernatant was treated with C-ABC and chondroitinase AC-II. The sample was ultrafiltered and the unsaturated disaccharides 2-acetamide-2-deoxy-3-*O*-(β-D-gluco-4-enepyranosyluronic acid)-D-galactose, 2-acetamide-2-deoxy-3-*O*-(β-D-gluco-4-enepyranosyluronic acid)-4-*O*-sulfo-D-galactose and 2-acetamide-2-deoxy-3-*O*-(β-D-gluco-4-enepyranosyluronic acid)-6-*O*-sulfo-D-galactose derived from chondroitin sulfate in the filtrate were analysed by HPLC. The disaccharides in each sample were eluted with a gradient of 0–100 mM sodium sulfate and the effluent was monitored using a fluoro-monitor. The amount of each unsaturated disaccharide was calculated from the peak area and the contents of these isomers per unit weight of spinal cord were investigated.

Immunohistochemistry

The animals were deeply anesthetized by the inhalation of diethyl ether and intracardially perfused with 4% paraformaldehyde in 0.1 M phosphate-buffered saline. Tissue samples were immersed in 10% sucrose in phosphate-buffered saline at 4 °C for 24 h, placed in 30% sucrose in phosphate-buffered saline for 48 h and embedded in optimal cutting temperature compound. The embedded tissue was immediately frozen in liquid nitrogen and cut into 30-μm sagittal sections. For the immunofluorescence staining, the sections were incubated at 4 °C overnight with the following primary antibodies: anti-GFP antibody (rabbit polyclonal, 1 : 400; MBL), anti-CSPG antibody (CS56, mouse monoclonal IgM, 1 : 100; Sigma) and anti-neurofilament antibody (RT97, mouse monoclonal, 1 : 10; Chemicon). After washing with phosphate-buffered saline, the sections were incubated with appropriate secondary antibodies (Alexa Fluor 488 anti-rabbit IgG, 1 : 1000; 568 anti-mouse IgM, 1 : 1000; 350 anti-

mouse IgG, 1 : 1000; Molecular Probes) at room temperature for 1 h. For diaminobenzidine (Sigma) staining, the endogenous peroxidase activity was blocked with 3% hydrogen peroxide and the sections were incubated at 4 °C overnight using the following primary antibodies: anti-CSPG antibody (CS56, 1 : 100), anti-proteoglycan 2-acetamide-2-deoxy-3-*O*-(β-D-gluco-4-enepyranosyluronic acid)-4-*O*-sulfo-D-galactose antibody (2B6, mouse monoclonal, 1 : 100; Seikagaku) and anti-growth-associated protein-43 (GAP-43) antibody (MAB347, mouse monoclonal, 1 : 500; Chemicon) followed by horseradish peroxidase-labeled goat anti-mouse IgM or IgG secondary antibodies (1 : 1000; Jackson ImmunoResearch, West Grove, PA, USA). Staining was visualized with diaminobenzidine and the slides were washed, dehydrated, cleared in xylene and mounted. The stained sections were examined under a microscope (Axioskop 2 plus, Carl Zeiss), except for those used to quantify the GAP-43-positive fibers.

Quantification of growth-associated protein-43-positive fibers

To quantify the GAP-43-positive fibers *in vivo*, sagittal sections from each group (C-ABC infusion plus NSPC transplantation group, $n = 14$; inactivated C-ABC infusion plus NSPC transplantation group, $n = 7$; inactivated C-ABC infusion plus medium injection group, $n = 5$) immunostained with anti-GAP-43 antibody were analysed using the MCID system equipped with a CCD camera (DXC-390, Sony, Tokyo, Japan). The median section of the injured spinal cord was scanned transversely throughout a cephalocaudal length of 175 μm, including the lesion epicentre. The immunopositive fibers were identified on the transversely tiled images and the total positive area was measured.

Statistical analysis

All data were reported as the mean ± SEM. The results of the migration and HPLC assays were analysed for statistical significance using a one-way ANOVA with a Fisher post-hoc test. The results of the survival and differentiation assays were analysed by an unpaired *t*-test. The quantified GAP-43-positive fiber area was analysed by a Kruskal–Wallis test. In all analyses, statistical significance was accepted at a P-value < 0.05.

Results

Effects of chondroitin sulfate proteoglycan and chondroitinase ABC on the migration, survival and differentiation of neural stem/progenitor cells

We investigated the migration of NSPC-derived cells from the original neurospheres plated in laminin-coated wells and CSPG-coated wells that were treated with or without C-ABC *in vitro*. Neurospheres plated in each well attached within 1 h and migrating cells started to become apparent on the periphery of the attached neurosphere. In the laminin-coated wells, a number of cells migrated far (154.3 ± 3.9 μm) from the neurosphere uniformly in all directions (Fig. 1, A1). In the CSPG-coated wells, a very small number of cells migrated slightly, forming small clusters of cells around the periphery of the attached neurosphere (Fig. 1, B1). The average migration distance of the cells from the neurospheres in the CSPG-coated wells (35.9 ± 2.3 μm) was significantly shorter than that of the cells plated in the laminin-coated wells. In contrast, a number of cells migrated away from the neurospheres in the C-ABC-treated wells (Fig. 1, C1). The average migration distance of the cells from the neurospheres in the C-ABC-treated wells (127.2 ± 4.3 μm) was significantly longer than that of the cells in the CSPG-coated wells (Fig. 1D). Immunocytochemistry for nestin revealed that most of the migrating cells in each substrate were nestin-positive (Fig. 1, A4, B4 and C4). The survival assay using bioluminescence showed no significant difference in the viability of NSPCs cultured in laminin-coated wells and those cultured in CSPG-coated wells (Fig. 1E). Furthermore, to determine the effect of CSPG on the differentiation of NSPCs *in vitro*, we performed a differentiation assay. The morphologies of each type of differentiated cells, such as neurons, astrocytes and oligodendrocytes, on each substrate were similar (Fig. 1F–H). A quantitative analysis revealed no significant differences in the proportions of each cell type in the laminin-coated and the CSPG-coated wells (Fig. 1I).

Chondroitin sulfate proteoglycan immunoreactivity peaked within 2 weeks after spinal cord injury

To determine the appropriate period for applying C-ABC to injured spinal cord *in vivo*, we examined the immunoreactivity of CSPG within the injured spinal cord. As an SCI model, spinal contusion lesions were made in accordance with the MASCIS method using an NYU impactor (Gruner, 1992) in adult female Sprague-Dawley rats. As the contusive SCI model created by an NYU impactor is well-established and reproducible, it is used for histological and/or behavioral analysis of injured spinal cord (Basso *et al.*, 1996; Beattie *et al.*, 1997; Metz *et al.*, 2000). In this model, while immunoreactivity of CSPG was low in intact spinal cord (Fig. 2A), increased immunoreactivity was observed in the area surrounding the lesion at 4 days after injury (Fig. 2B, arrows). By 2 weeks after injury, high and diffuse CSPG immunoreactivity was observed at the lesion site (Fig. 2C, arrows) and the immunoreactivity remained highly elevated for 4 weeks after injury (Fig. 2D, arrows). At 8 weeks after injury, the injured spinal cord appeared atrophic and CSPG immunoreactivity at the lesion site was lower than the levels observed at earlier time points (Fig. 2E). A negative control without the primary antibody exhibited only a low level of background staining (Fig. 2F).

Continuous application of chondroitinase ABC digested chondroitin sulfate proteoglycan within the injured spinal cord

Based on the finding that CSPG immunoreactivity within the spinal cord peaked at 2 weeks after SCI, we used an osmotic pump to infuse C-ABC continuously from 1 to 2 weeks after SCI to digest the CSPG within the injured spinal cord. To evaluate the change in C-ABC activity in the osmotic pump, we incubated C-ABC solution (200 U/mL) *ex vivo* with polymeric beads made of the same materials as the pump reservoir for 7 days and measured the remaining C-ABC activity, which decreased to 51.0 ± 1.8% of the pre-incubation activity level (Fig. 3). This result suggested that about 50% of the C-ABC activity was maintained in the osmotic pump after 7 days. Using this osmotic pump, we then continuously infused C-ABC into the subarachnoid space adjacent to the lesion site from 1 to 2 weeks after SCI to determine whether C-ABC could digest CSPG within the injured spinal cord. CSPG immunoreactivity of the injured spinal cord decreased after C-ABC (Fig. 4A) but not after inactivated C-ABC (Fig. 4C) infusion. Consistently, high immunoreactivity with 2B6, an antibody against digested stubs of chondroitin sulfate, within the injured spinal cord was observed after C-ABC (Fig. 4B) but not after inactivated C-ABC (Fig. 4D) infusion. Furthermore, we quantified the amount of CSPG within the injured spinal cord tissue using HPLC. The amount of CSPG in the injured spinal cord treated with inactivated C-ABC was twice that

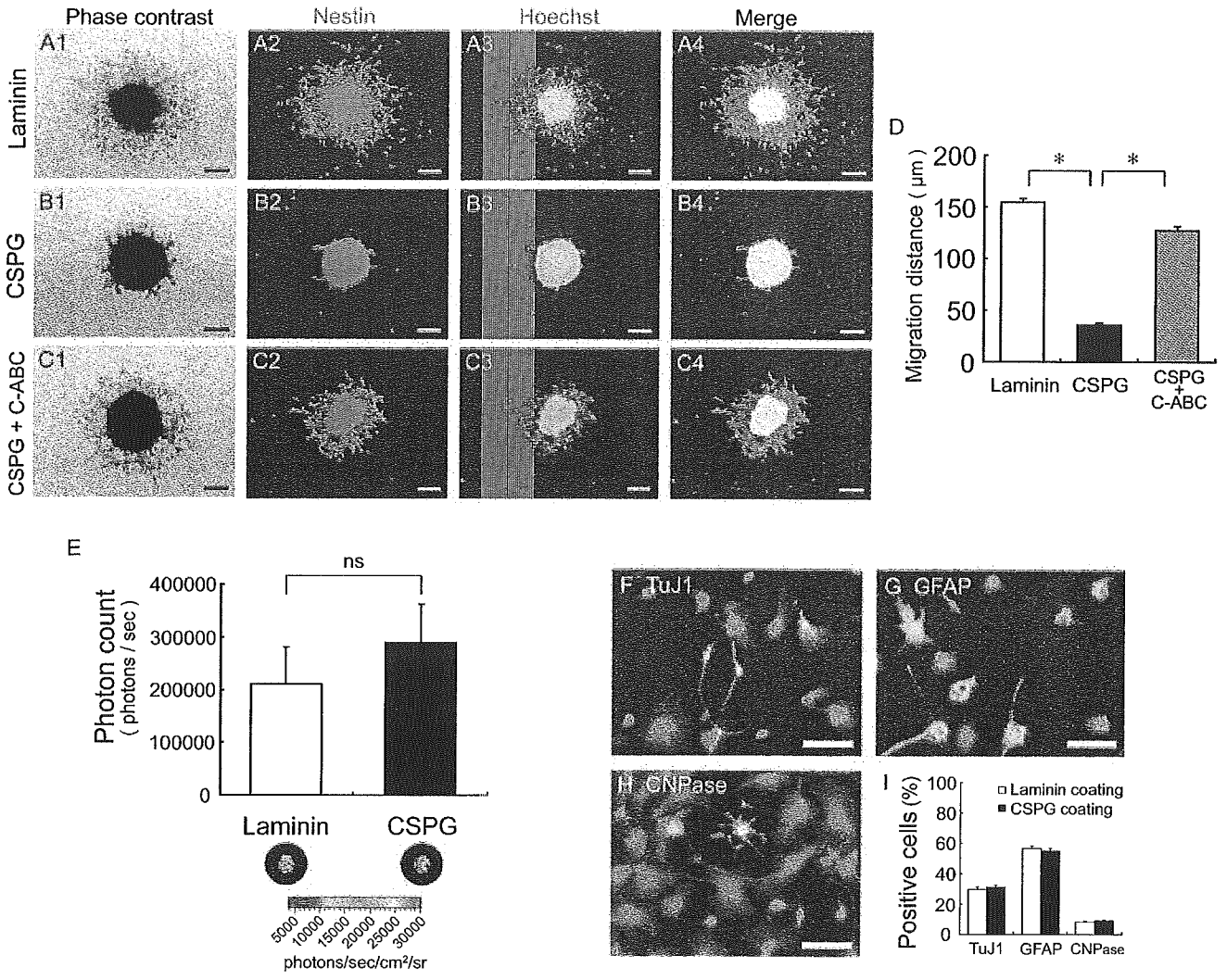

FIG. 1. (A–D) Migration assay. Neurospheres were plated and cultured in laminin- (A) and chondroitin sulfate proteoglycan (CSPG)-coated wells without (B) and with (C) chondroitinase ABC (C-ABC) treatment. Cell migration was inhibited in the CSPG-coated wells (B), compared with that in the laminin-coated wells (A). However, this inhibitory effect of CSPG on cell migration was attenuated by C-ABC treatment (C and D). Nestin expression (A2, B2 and C2) and nuclear counterstaining with Hoechst (A3, B3 and C3) in cells incubated on each of the indicated substrates are shown. Merged images of nestin and Hoechst staining (A4, B4 and C4) show that most of the migrating cells on each substrate were nestin-positive. (E) Survival assay. Genetically modified neurospheres transduced by lentiviruses to express luciferase were plated in laminin- or CSPG-coated wells. The photon count from each well was in direct proportion to the cell viability. No significant difference was observed between the viabilities of neural stem/progenitor cells (NSPCs) cultured in the laminin- and the CSPG-coated wells. (F–I) Differentiation assay. Single NSPCs derived from green rats were cultured in laminin- or CSPG-coated wells for 4 days and double-immunostained with anti-green fluorescent protein antibody and markers for each phenotype. TuJ1 (F), glial fibrillary acidic protein (GFAP) (G) and 2′3′-cyclic nucleotide 3′-phosphodiesterase (CNPase) (H)-positive cells in laminin-coated wells are shown. No significant differences in the proportions of each cell type were observed between the laminin- and the CSPG-coated wells (I). Values are the mean ± SEM. $*P < 0.05$. Scale bars, 100 μm (A–C) and 50 μm (F–H).

in the intact spinal cord. In contrast, C-ABC treatment decreased the amount of CSPG to the level seen in intact spinal cord (Fig. 4E). Taken together, these results suggest that the continuous application of C-ABC to the subarachnoid space from 1 to 2 weeks after SCI could effectively digest CSPG in the injured spinal cord *in vivo*.

Chondroitinase ABC treatment attenuated the inhibitory effect of chondroitin sulfate proteoglycan on neural stem/progenitor cell migration in vivo

To examine the effect of C-ABC on the migration of NSPCs *in vivo*, we transplanted NSPCs derived from green rats into the lesion epicentre of injured spinal cord just after C-ABC or inactivated C-ABC infusion. After inactivated C-ABC infusion, strong and extensive CSPG immunoreactivity was observed at the lesion epicentre. Interestingly, in this CSPG-rich area, the migration of transplanted cells into the host spinal cord (Fig. 5A) and the interaction of these GFP-positive cells with neurofilament (RT97)-positive fibers were inhibited at the lesion epicentre (Fig. 5B). In contrast, C-ABC application reduced the CSPG immunoreactivity of the injured spinal cord and resulted in the further migration of the transplanted cells mainly into the white matter of the injured spinal cord, compared with the situation seen after the application of inactivated C-ABC. Notably, transplant-derived cells integrated well into the host spinal cord parenchyma, with numerous processes (arrows in Fig. 5C) avoiding CSPG-rich tissue. These migrating cells

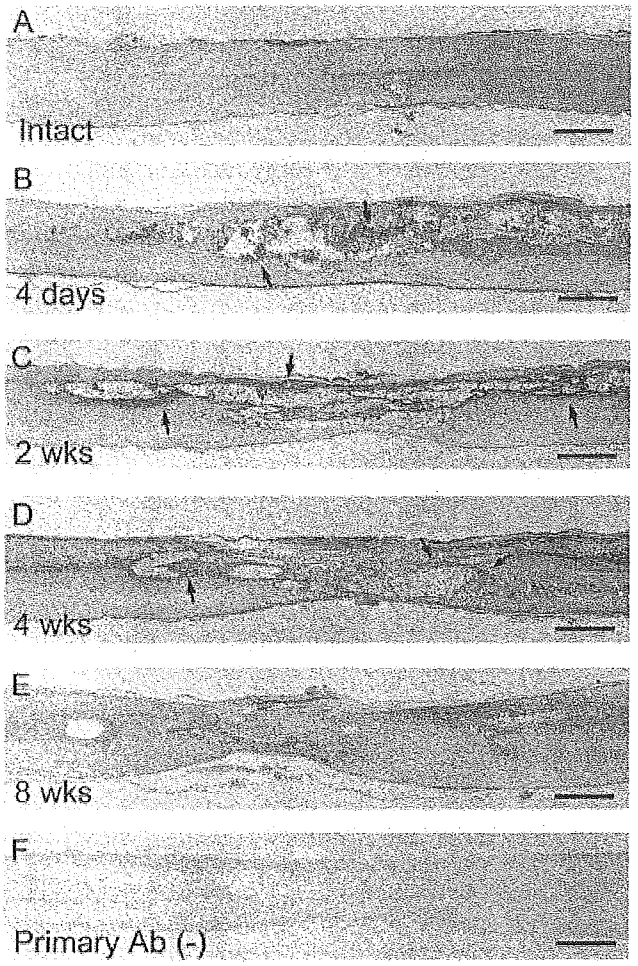

FIG. 2. Time course of chondroitin sulfate proteoglycan (CSPG) expression after spinal cord injury (SCI). (A) CSPG was expressed at low levels in the intact spinal cord. (B) At 4 days after SCI, immunoreactivity of CSPG (arrows) was visible at the lesion site. (C and D) Strong immunoreactivity of CSPG was observed around the cavity at the lesion site (arrows) from 2 to 4 weeks after injury. (E) At 8 weeks after injury, the immunoreactivity of CSPG at the lesion site was reduced, compared with observations at earlier time points. (F) Primary antibody omission control. Scale bars, 1 mm.

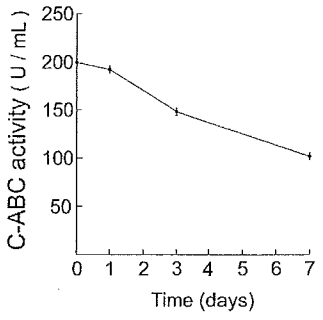

FIG. 3. *Ex vivo* measurement of chondroitinase ABC (C-ABC) activity. C-ABC solution (200 U/mL) was incubated *ex vivo* with polymeric beads made of the same materials as the pump reservoir and the remaining C-ABC activity was progressively measured at 0, 1, 3 and 7 days after the beginning of incubation. C-ABC activity decreased to about 50% after 7 days. Values are the mean ± SEM.

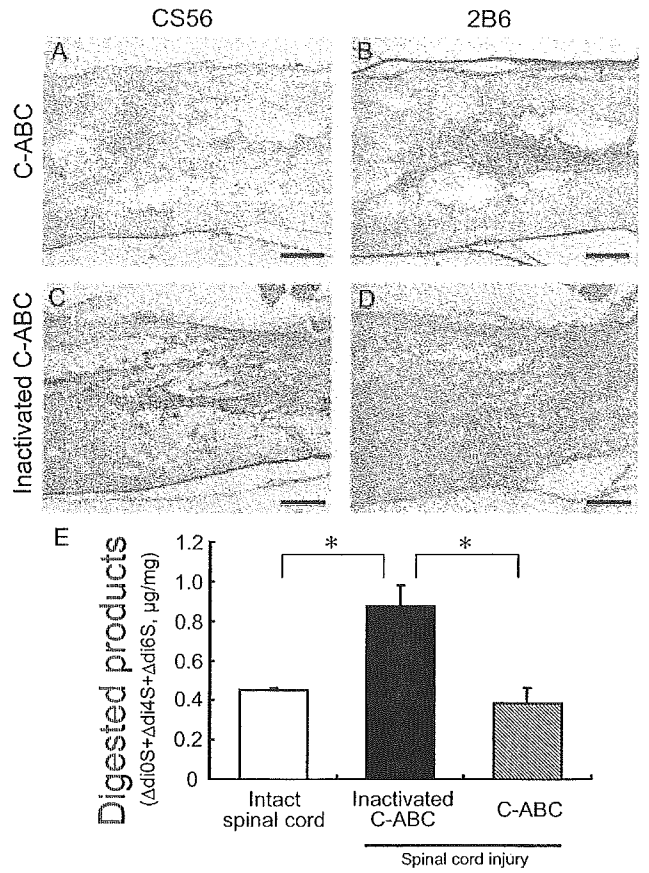

FIG. 4. Continuous chondroitinase ABC (C-ABC) infusion into the subarachnoid space resulted in the effective digestion of chondroitin sulfate proteoglycan (CSPG). Immunohistochemistry with CS56 (A and C) or 2B6 (B and D) antibodies in adjacent sections of the injured spinal cord after C-ABC (A and B) or inactivated C-ABC (C and D) infusion. CS56 immunoreactivity in the injured spinal cord decreased after C-ABC infusion (A) but not after inactivated C-ABC infusion (C). In contrast, a strong immunoreactivity with 2B6 was observed at the lesion site after C-ABC infusion (B) but not after inactivated C-ABC infusion (D). (E) The injured spinal cord after C-ABC or inactivated C-ABC infusion was removed and thoroughly digested by C-ABC *ex vivo*. Digested products [2-acetamide-2-deoxy-3-*O*-(β-D-gluco-4-enepyranosyluronic acid)-D-galactose (Δdi0S) + 2-acetamide-2-deoxy-3-*O*-(β-D-gluco-4-enepyranosyluronic acid)-4-*O*-sulfo-D-galactose (Δdi4S) + 2-acetamide-2-deoxy-3-*O*-(β-D-gluco-4-enepyranosyluronic acid)-6-*O*-sulfo-D-galactose (Δdi6S)] were quantified using high-performance liquid chromatography. These products were in direct proportion to the amount of CSPG remaining in the injured spinal cord after C-ABC or inactivated C-ABC infusion. The amount of CSPG in the injured spinal cord after inactivated C-ABC infusion, which was twice that in the intact spinal cord, decreased to the level of the intact spinal cord after C-ABC infusion. Values are the mean ± SEM. $*P < 0.05$. Scale bars, 500 μm.

became aligned along the neurofilament-positive fibers in the spared white matter and were also in contact with the neurofilament-positive fibers of the host spinal cord (Fig. 5D).

Combined treatment of chondroitinase ABC application and neural stem/progenitor cell transplantation promoted outgrowth of growth-associated protein-43-positive fibers in the injured spinal cord

To determine the effect of the combination of C-ABC application and NSPC transplantation on the axonal regeneration of the host spinal

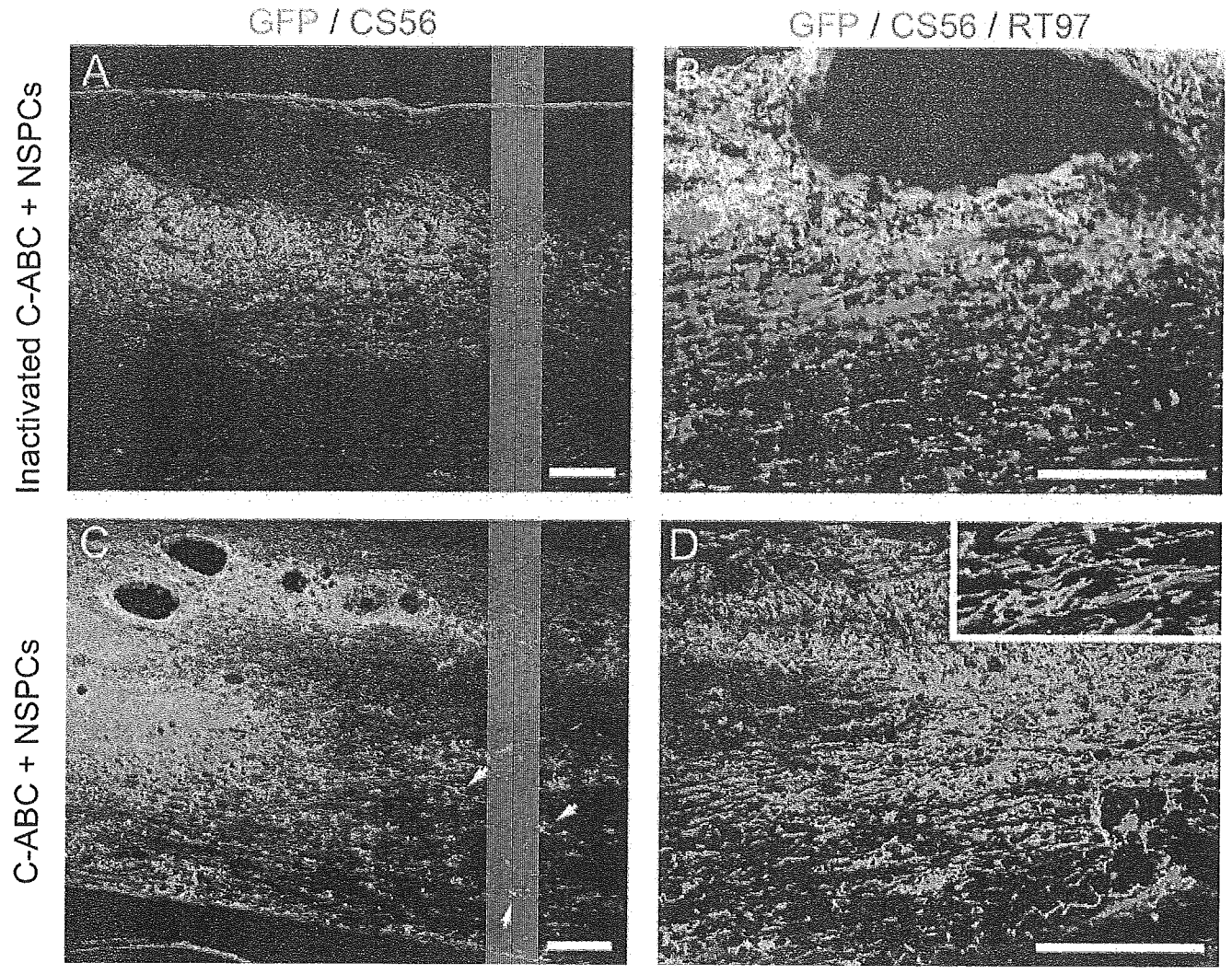

FIG. 5. Chondroitinase ABC (C-ABC) attenuated the inhibitory effect of chondroitin sulfate proteoglycan (CSPG) on neural stem/progenitor cell (NSPC) migration *in vivo* and promoted the interaction between the transplanted cells and the axons of host spinal cord. (A) NSPCs (green) transplanted into injured spinal cord after inactivated C-ABC infusion were surrounded with CSPG-rich tissue (red). This CSPG barrier prevented further migration of the transplanted cells. (B) Most of the transplanted cells adhered to the cavity wall and could not interact with neurofilament (RT97)-positive fibers (blue). (C) After C-ABC intrathecal infusion, CSPG immunoreactivity decreased and some of the transplant-derived cells migrated extensively into the white matter of the injured spinal cord and integrated successfully into surrounding tissue (arrows), avoiding CSPG-rich tissue. (D) These migrating cells were aligned along RT97-positive fibers (blue) of the host spinal cord and seemed to interact with these fibers. Scale bars, 200 μm. GFP, green fluorescent protein.

cord, we quantified the GAP-43-positive regenerating axons at the lesion epicentre after each treatment. Median frozen sections from each group (C-ABC plus NSPCs, $n = 14$; inactivated C-ABC plus NSPCs, $n = 7$; inactivated C-ABC plus medium, $n = 5$) were immunostained with anti-GAP-43 antibody and the positive fibers were quantified. In each group, the dorsal column of the spinal cord was usually more affected by the contusion than the ventral column and more GAP-43-positive fibers were observed in the ventral than in the dorsal column. In the vehicle group (inactivated C-ABC plus medium), few GAP-43-positive fibers were observed at the lesion epicentre (Fig. 6A). While the GAP-43-positive fibers that regrew in the lesion epicentre were scattered, thin and relatively unbranched in the animals that received inactivated C-ABC and NSPC transplantation (Fig. 6B), the pattern of axonal growth was denser with more branching at the lesion epicentre in the animals that received C-ABC and NSPC transplantation (Fig. 6C). Quantitative analysis of the GAP-43-positive fibers by MCID (Fig. 6D, computer-analysed image of Fig. 6C) revealed significant differences in the total areas of the GAP-43-positive fibers among the three groups (Fig. 6E).

Discussion

Chondroitinase ABC attenuated the inhibitory effect of chondroitin sulfate proteoglycan on neural stem/progenitor cell migration in vitro

Recent studies have reported that CSPG inhibits neurite outgrowth and induces growth cone collapse (Snow *et al.*, 1990, 1991, 2001; Oohira *et al.*, 1991; Niederost *et al.*, 1999; Tisay & Key, 1999; Dillon *et al.*, 2000; Yu & Bellamkonda, 2001; Hynds & Snow, 2002; Monnier *et al.*, 2003; Ughrin *et al.*, 2003). However, few reports have investigated the effects of CSPG on cell motility (Landolt *et al.*, 1995; Kearns *et al.*,

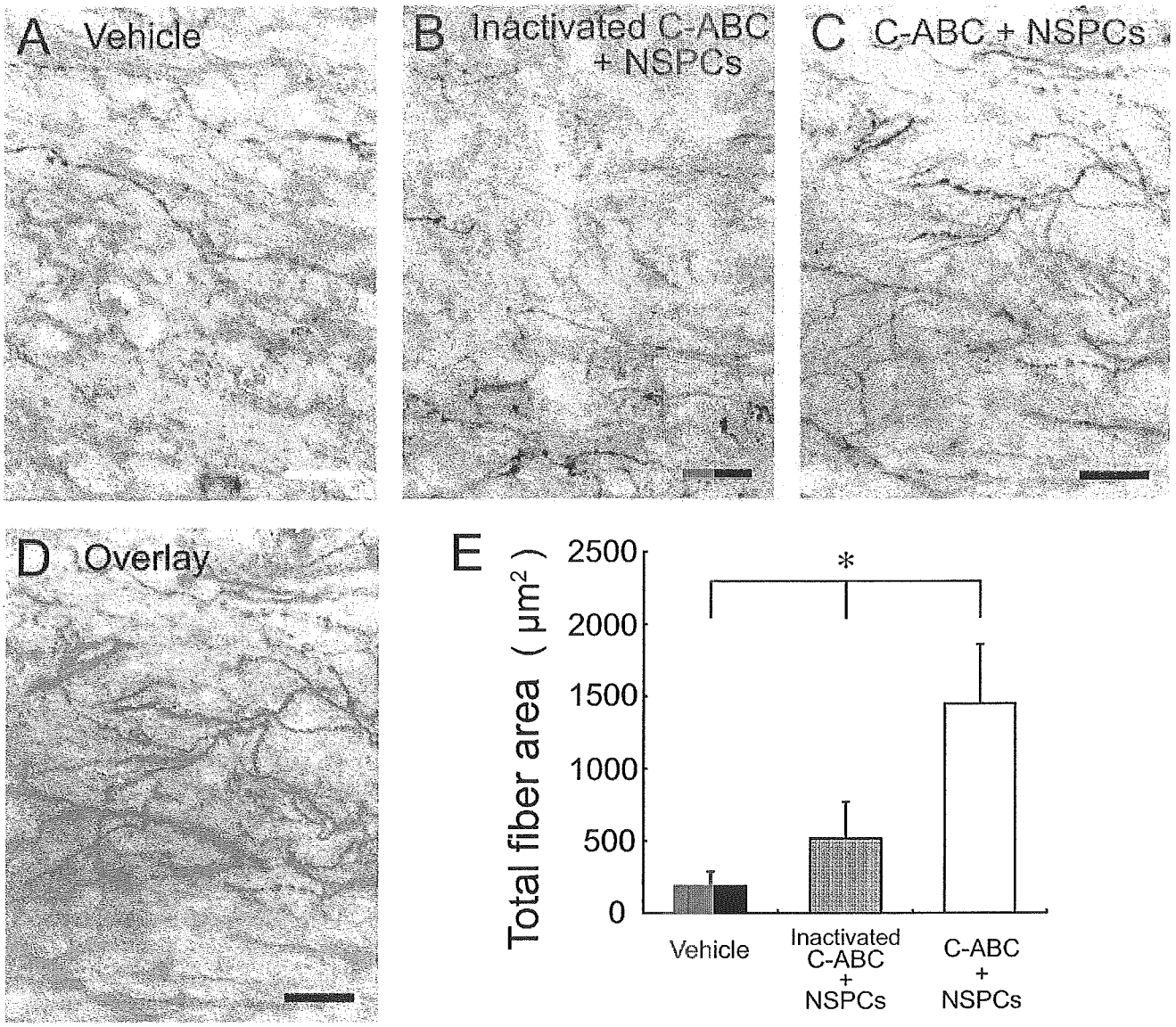

FIG. 6. The combination of chondroitinase ABC (C-ABC) application and neural stem/progenitor cell (NSPC) transplantation promoted the outgrowth of growth-associated protein-43 (GAP-43)-positive fibers in the injured spinal cord. Transverse sections stained with anti-GAP-43 antibody in the vehicle control animals (A), animals treated with inactivated C-ABC plus NSPC transplantation (B) and animals treated with C-ABC plus NSPC transplantation (C). The total area of GAP-43-positive fibers was quantified (D). Significant differences in the areas of the GAP-43-positive fibers were observed among the three groups (E). Values are the mean ± SEM. $*P < 0.05$. Scale bars, 30 μm.

2003). In the present study, to investigate the effect of CSPG on NSPC migration *in vivo*, we performed an *in vitro* migration assay mimicking the environment of the injured spinal cord (Fig. 1A–D). The CSPG mixture which we used for coating *in vitro* was derived from embryonic chicken brains and consisted chiefly of neurocan, phosphacan, versican and aggrecan, which resembles the CSPG expression profile within injured spinal cord (Henke-Fahle *et al.*, 2001; Jones *et al.*, 2003; Tang *et al.*, 2003). Kearns *et al.* (2003) demonstrated that CSPG significantly inhibited the migratory outgrowth and velocity of cells from the original neurosphere. In the present study, we showed that the migration distance of nestin-positive immature cells from neurospheres in CSPG-coated wells was significantly less than that in laminin-coated wells, agreeing with the conclusion of a previous report (Kearns *et al.*, 2003). Furthermore, we demonstrated that the cells recovered their migration ability in CSPG-coated wells that were pre-treated with C-ABC before plating (Fig. 1D). These findings implied that CSPG inhibited the migration of NSPC-derived cells and that C-ABC neutralized this effect *in vitro*. We next sought to rule out the possibility that CSPG affected the survival or differentiation of NSPCs. The survival and differentiation assays revealed that CSPG did not affect either the viability or differentiation of NSPCs (Fig. 1E–I). Taken together, these findings demonstrated that CSPG inhibited the migration of NSPCs and that C-ABC attenuated this inhibitory effect *in vitro*.

Continuous intrathecal infusion of chondroitinase ABC digested chondroitin sulfate proteoglycan within injured spinal cord

Several researchers have investigated the expression of CSPG in transected spinal cord using immunohistochemistry or western blot

analysis (Jones *et al.*, 2002, 2003; Tang *et al.*, 2003). However, only one report has described the change in CSPG expression after contusive SCI. Lemons *et al.* (1999) reported that the immunoreactivity of CSPG increased at 7 days after contusion injury and that the immunoreactivity in the ventral half of the white matter decreased at 30 and 40 days after injury. Consistently, in our present contusion SCI model, we found that CSPG immunoreactivity increased after contusion injury, peaking between 1 and 2 weeks after injury (Fig. 2). Therefore, we applied C-ABC solution continuously into the subarachnoid space using an osmotic pump during this time window. Bradbury *et al.* (2002) applied C-ABC (10 U/mL) intrathecally to dorsally hemisected spinal cord and confirmed the digestion of CSPG within the spinal cord parenchyma by immunostaining with 2B6 antibody. Compared with hemisection injuries, it may be difficult to deliver C-ABC to the spinal cord parenchyma after contusion injuries because the molecular weight of C-ABC is so large that C-ABC cannot pass through the pia mater. Moreover, C-ABC should be applied at a high concentration to avoid spontaneous degradation of C-ABC in the osmotic pump because the protein (e.g. enzyme) is generally more stable at high concentrations. Olmarker *et al.* (1996) reported that a single high-dose infusion of C-ABC (200 U/mL) into the subarachnoid space of a pig did not affect the conduction velocity or histology of lumbar nerve roots. Thus, we also applied C-ABC at a high concentration (200 U/mL) into the subarachnoid space using the osmotic pump. *Ex vivo* measurement of C-ABC activity using polymeric beads made of the same materials as the pump reservoir revealed that approximately 50% of C-ABC activity was maintained for 7 days (Fig. 3). Based on these results (application period, administration route and change in enzyme activity), we infused C-ABC (initial loading concentration 200 U/mL) continuously, using the osmotic pump, into the subarachnoid space in close proximity to the lesion site from 1 to 2 weeks after SCI. Immunohistochemical analysis (with CS56 and 2B6 antibodies) and HPLC assay revealed that the intrathecal application of C-ABC digested CSPG within the injured spinal cord and decreased the amount of CSPG to the level observed in intact spinal cord (Fig. 4).

Chondroitinase ABC attenuated the inhibitory effect of chondroitin sulfate proteoglycan on neural stem/progenitor cell migration in vivo

We previously showed that the transplantation of NSPCs into injured spinal cord can contribute to the repair of injured spinal cord in adult rats (Ogawa *et al.*, 2002; Okano *et al.*, 2003; Watanabe *et al.*, 2004) and non-human primates (Iwanami *et al.*, 2005). However, in some cases, a large percentage of the transplanted cells adhered to the cavity wall and did not migrate into the host spinal cord. Generally, it is preferable that the transplanted cells migrate from the lesion epicentre into the host spinal cord parenchyma for the following two reasons. First, the environment in the lesion epicentre may be harmful for the transplanted cells because of poor blood circulation and an elevated internal pressure. Nornes *et al.* (1983) reported that a superior blood supply improved the survival of cells transplanted in the subpial location. Second, an insufficient integration between the transplanted cells and the host spinal cord may result in a limited anatomic and functional recovery after SCI (Predy & Malhotra, 1989; Grijalva *et al.*, 1996). Glial scar formation might obstruct adequate integration between the transplant and host tissues, thereby blocking the potentially beneficial effect of the transplant on functional recovery (Das, 1983; Nornes *et al.*, 1983; Houle & Reier, 1988; Reier *et al.*, 1988). We hypothesized that the digestion of CSPG, a constituent of glial scar tissue (Fitch & Silver, 1997; Lemons *et al.*, 1999; Jones *et al.*, 2002; Monnier *et al.*, 2003; Tang *et al.*, 2003; Yick *et al.*, 2003), by C-ABC might promote the migration of transplanted NSPC-derived cells into the host spinal cord parenchyma and improve integration between the transplanted cells and the host spinal cord. While cell migration was inhibited by CSPG-immunopositive scar tissue around the lesion cavity in the control animals, the pre-treatment of injured spinal cord by C-ABC promoted the migration of NSPC-derived cells (Fig. 5). Interestingly, these *in vivo* findings were consistent with the findings observed *in vitro*. The extensive migration of the transplanted NSPC-derived cells into host spinal cord parenchyma resulted in a close association between the transplanted cells and neurofilament-positive fibers, whereas the interaction between the transplanted cells and neurofilament-positive fibers was inhibited by CSPG-rich tissue in the inactivated C-ABC-infused rats. Moreover, the extensive migration of cells into the CSPG-diminished surrounding tissue suggests that these cells may be able to promote axonal regeneration of the host spinal cord.

Combined treatment of chondroitinase ABC application and neural stem/progenitor cell transplantation promoted outgrowth of growth-associated protein-43-positive fibers in the injured spinal cord

Several researchers have reported that C-ABC promotes axonal regeneration *in vitro* (Zuo *et al.*, 1998; Niederost *et al.*, 1999) and *in vivo* (Yick *et al.*, 2000, 2003, 2004; Bradbury *et al.*, 2002; Chau *et al.*, 2004; Fouad *et al.*, 2005; reviewed by Silver & Miller, 2004). Consistent with this, we could also show that the inhibitory effect of CSPG on the neurite outgrowth of cerebellar granule neurons was attenuated by the application of C-ABC *in vitro* (data not shown). Based on these findings, we expected the combination of NSPC transplantation and C-ABC application to have a synergistic effect on putative neurite outgrowth *in vivo* after SCI. For this purpose, we examined the immunohistochemical staining of GAP-43, which had been used to detect regenerating axons or neurite extensions in the previous studies (Schreyer & Skene, 1991; Li *et al.*, 1996; Kobayashi *et al.*, 1997; Brook *et al.*, 1998; Ramon-Cueto *et al.*, 1998; Teng *et al.*, 2002; Kim & Jahng, 2004). In the present study, we showed that there was a significant difference in the area of GAP-43-positive fibers at the lesion epicentre among the three groups: C-ABC plus NSPC-treated rats, NSPC-treated rats and vehicle controls (Fig. 6). The synergistic effect of the combination of C-ABC application and NSPC transplantation on the outgrowth of GAP-43-positive fibers after SCI might be attributed to different mechanisms. While C-ABC application promoted axonal regeneration by digesting CSPG, a known inhibitory molecule for axonal regeneration (Yick *et al.*, 2000; Bradbury *et al.*, 2002; Chau *et al.*, 2004), NSPC transplantation might promote axonal regeneration or neurite outgrowth by secreting neurotrophic factors, remyelinating or reconnecting the disrupted neuronal circuit (Blesch *et al.*, 2002; Ogawa *et al.*, 2002; Lu *et al.*, 2003; Llado *et al.*, 2004).

In conclusion, this is the first study to demonstrate that CSPG inhibited NSPC migration and that C-ABC attenuated this inhibitory effect both *in vitro* and *in vivo*. The transplanted NSPCs migrated extensively into injured spinal cord pre-treated with C-ABC and associated closely with neurofilament-positive fibers. The combination of C-ABC application and NSPC transplantation putatively induced the neurite outgrowth *in vivo* in the form of GAP-43-positive fibers and may be a promising regeneration strategy.

Acknowledgements

We appreciate the help of the members of the Okano Laboratory at the Department of Physiology, Keio University School of Medicine, the spinal cord investigation team at the Department of Orthopaedic Surgery, Keio University School of Medicine and Seikagaku Corporation. We also thank Ms S. Miyao and Ms T. Harada for their assistance with the experiments and care of the animals. This work was supported by grants from the Japan Science and Technology Agency, Core Research for Evolutional Science and Technology, a Grant-in-Aid for the 21st Century Center of Excellence program to Keio University from the Japanese Ministry of Education, Culture, Sports, Science and Technology, a Grant-in-Aid for scientific research to M.N. from the Japanese Ministry of Education, Culture, Sports, Science and Technology and a grant from the General Insurance Association of Japan.

Abbreviations

C-ABC, chondroitinase ABC; CSPG, chondroitin sulfate proteoglycan; GAP-43, growth-associated protein-43; GFP, green fluorescent protein; HPLC, high-performance liquid chromatography; NSPC, neural stem/progenitor cell; SCI, spinal cord injury.

References

Basso, D.M., Beattie, M.S. & Bresnahan, J.C. (1996) Graded histological and locomotor outcomes after spinal cord contusion using the NYU weight-drop device versus transection. *Exp. Neurol.*, **139**, 244–256.

Beattie, M.S., Bresnahan, J.C., Komon, J., Tovar, C.A., Van Meter, M., Anderson, D.K., Faden, A.I., Hsu, C.Y., Noble, L.J., Salzman, S. & Young, W. (1997) Endogenous repair after spinal cord contusion injuries in the rat. *Exp. Neurol.*, **148**, 453–463.

Blesch, A., Lu, P. & Tuszynski, M.H. (2002) Neurotrophic factors, gene therapy, and neural stem cells for spinal cord repair. *Brain Res. Bull.*, **57**, 833–838.

Bradbury, E.J., Moon, L.D., Popat, R.J., King, V.R., Bennett, G.S., Patel, P.N., Fawcett, J.W. & McMahon, S.B. (2002) Chondroitinase ABC promotes functional recovery after spinal cord injury. *Nature*, **416**, 636–640.

Brook, G.A., Plate, D., Franzen, R., Martin, D., Moonen, G., Schoenen, J., Schmitt, A.B., Noth, J. & Nacimiento, W. (1998) Spontaneous longitudinally orientated axonal regeneration is associated with the Schwann cell framework within the lesion site following spinal cord compression injury of the rat. *J. Neurosci. Res.*, **53**, 51–65.

Chau, C.H., Shum, D.K., Li, H., Pei, J., Lui, Y.Y., Wirthlin, L., Chan, Y.S. & Xu, X.M. (2004) Chondroitinase ABC enhances axonal regrowth through Schwann cell-seeded guidance channels after spinal cord injury. *Faseb J.*, **18**, 194–196.

Contag, C.H. & Bachmann, M.H. (2002) Advances in in vivo bioluminescence imaging of gene expression. *Annu. Rev. Biomed. Eng.*, **4**, 235–260.

Das, G.D. (1983) Neural transplantation in the spinal cord of adult rats. Conditions, survival, cytology and connectivity of the transplants. *J. Neurol. Sci.*, **62**, 191–210.

Dillon, G.P., Yu, X. & Bellamkonda, R.V. (2000) The polarity and magnitude of ambient charge influences three-dimensional neurite extension from DRGs. *J. Biomed. Mat. Res.*, **51**, 510–519.

Fitch, M.T. & Silver, J. (1997) Glial cell extracellular matrix: boundaries for axon growth in development and regeneration. *Cell Tissue Res.*, **290**, 379–384.

Fouad, K., Schnell, L., Bunge, M.B., Schwab, M.E., Liebscher, T. & Pearse, D.D. (2005) Combining Schwann cell bridges and olfactory-ensheathing glia grafts with chondroitinase promotes locomotor recovery after complete transection of the spinal cord. *J. Neurosci.*, **25**, 1169–1178.

Grijalva, I., Guizar-Sahagun, G., Salgado-Ceballos, H., Ibarra, A., Franco-Bourland, R., Espitia, L. & Madrazo, I. (1996) Improvement of host-graft adhesion by enzymatic manipulation of the subacute spinal cord contusion area in the rat. *Transplant Proc.*, **28**, 3340–3342.

Gruner, J.A. (1992) A monitored contusion model of spinal cord injury in the rat. *J. Neurotrauma*, **9**, 123–126; discussion 126–128.

Henke-Fahle, S., Wild, K., Sierra, A. & Monnier, P.P. (2001) Characterization of a new brain-derived proteoglycan inhibiting retinal ganglion cell axon outgrowth. *Mol. Cell Neurosci.*, **18**, 541–556.

Houle, J.D. & Reier, P.J. (1988) Transplantation of fetal spinal cord tissue into the chronically injured adult rat spinal cord. *J. Comp. Neurol.*, **269**, 535–547.

Hynds, D.L. & Snow, D.M. (2002) A semi-automated image analysis method to quantify neurite preference/axon guidance on a patterned substratum. *J. Neurosci. Meth.*, **121**, 53–64.

Ito, T., Suzuki, A., Imai, E., Okabe, M. & Hori, M. (2001) Bone marrow is a reservoir of repopulating mesangial cells during glomerular remodeling. *J. Am. Soc. Nephrol.*, **12**, 2625–2635.

Iwanami, A., Kaneko, S., Nakamura, M., Kanemura, Y., Mori, H., Kobayashi, S., Yamasaki, M., Momoshima, S., Ishii, H., Ando, K., Tanioka, Y., Tamaoki, N., Nomura, T., Toyama, Y. & Okano, H. (2005) Transplantation of human neural stem cells for spinal cord injury in primates. *J. Neurosci. Res.*, **80**, 182–190.

Jones, L.L., Yamaguchi, Y., Stallcup, W.B. & Tuszynski, M.H. (2002) NG2 is a major chondroitin sulfate proteoglycan produced after spinal cord injury and is expressed by macrophages and oligodendrocyte progenitors. *J. Neurosci.*, **22**, 2792–2803.

Jones, L.L., Margolis, R.U. & Tuszynski, M.H. (2003) The chondroitin sulfate proteoglycans neurocan, brevican, phosphacan, and versican are differentially regulated following spinal cord injury. *Exp. Neurol.*, **182**, 399–411.

Kearns, S.M., Laywell, E.D., Kukekov, V.K. & Steindler, D.A. (2003) Extracellular matrix effects on neurosphere cell motility. *Exp. Neurol.*, **182**, 240–244.

Kim, D.H. & Jahng, T.A. (2004) Continuous brain-derived neurotrophic factor (BDNF) infusion after methylprednisolone treatment in severe spinal cord injury. *J. Korean Med. Sci.*, **19**, 113–122.

Kobayashi, N.R., Fan, D.P., Giehl, K.M., Bedard, A.M., Wiegand, S.J. & Tetzlaff, W. (1997) BDNF and NT-4/5 prevent atrophy of rat rubrospinal neurons after cervical axotomy, stimulate GAP-43 and Talpha1-tubulin mRNA expression, and promote axonal regeneration. *J. Neurosci.*, **17**, 9583–9595.

Landolt, R.M., Vaughan, L., Winterhalter, K.H. & Zimmermann, D.R. (1995) Versican is selectively expressed in embryonic tissues that act as barriers to neural crest cell migration and axon outgrowth. *Development*, **121**, 2303–2312.

Lemons, M.L., Howland, D.R. & Anderson, D.K. (1999) Chondroitin sulfate proteoglycan immunoreactivity increases following spinal cord injury and transplantation. *Exp. Neurol.*, **160**, 51–65.

Li, G.L., Farooque, M., Holtz, A. & Olsson, Y. (1996) Increased expression of growth-associated protein 43 immunoreactivity in axons following compression trauma to rat spinal cord. *Acta Neuropathol. (Berl.)*, **92**, 19–26.

Llado, J., Haenggeli, C., Maragakis, N.J., Snyder, E.Y. & Rothstein, J.D. (2004) Neural stem cells protect against glutamate-induced excitotoxicity and promote survival of injured motor neurons through the secretion of neurotrophic factors. *Mol. Cell Neurosci.*, **27**, 322–331.

Lu, P., Jones, L.L., Snyder, E.Y. & Tuszynski, M.H. (2003) Neural stem cells constitutively secrete neurotrophic factors and promote extensive host axonal growth after spinal cord injury. *Exp. Neurol.*, **181**, 115–129.

Metz, G.A., Curt, A., van de Meent, H., Klusman, I., Schwab, M.E. & Dietz, V. (2000) Validation of the weight-drop contusion model in rats: a comparative study of human spinal cord injury. *J. Neurotrauma*, **17**, 1–17.

Monnier, P.P., Sierra, A., Schwab, J.M., Henke-Fahle, S. & Mueller, B.K. (2003) The Rho/ROCK pathway mediates neurite growth-inhibitory activity associated with the chondroitin sulfate proteoglycans of the CNS glial scar. *Mol. Cell Neurosci.*, **22**, 319–330.

Niederost, B.P., Zimmermann, D.R., Schwab, M.E. & Bandtlow, C.E. (1999) Bovine CNS myelin contains neurite growth-inhibitory activity associated with chondroitin sulfate proteoglycans. *J. Neurosci.*, **19**, 8979–8989.

Nornes, H., Bjorklund, A. & Stenevi, U. (1983) Reinnervation of the denervated adult spinal cord of rats by intraspinal transplants of embryonic brain stem neurons. *Cell Tissue Res.*, **230**, 15–35.

Ogawa, Y., Sawamoto, K., Miyata, T., Miyao, S., Watanabe, M., Nakamura, M., Bregman, B.S., Koike, M., Uchiyama, Y., Toyama, Y. & Okano, H. (2002) Transplantation of in vitro-expanded fetal neural progenitor cells results in neurogenesis and functional recovery after spinal cord contusion injury in adult rats. *J. Neurosci. Res.*, **69**, 925–933.

Okada, S., Ishii, K., Yamane, J., Iwanami, A., Ikegami, T., Katoh, H., Iwamoto, Y., Nakamura, M., Miyoshi, H., Okano, H.J., Contag, C.H., Toyama, Y. & Okano, H. (2005) In vivo imaging of engrafted neural stem cells: its application in evaluating the optimal timing of transplantation for spinal cord injury. *FASEB J.*, **19**, 1839–1841.

Okano, H., Ogawa, Y., Nakamura, M., Kaneko, S., Iwanami, A. & Toyama, Y. (2003) Transplantation of neural stem cells into the spinal cord after injury. *Semin. Cell Dev. Biol.*, **14**, 191–198.

Olmarker, K., Stromberg, J., Blomquist, J., Zachrisson, P., Nannmark, U., Nordborg, C. & Rydevik, B. (1996) Chondroitinase ABC (pharmaceutical grade) for chemonucleolysis. Functional and structural evaluation after local

application on intraspinal nerve structures and blood vessels. *Spine*, **21**, 1952–1956.

Oohira, A., Matsui, F. & Katoh-Semba, R. (1991) Inhibitory effects of brain chondroitin sulfate proteoglycans on neurite outgrowth from PC12D cells. *J. Neurosci.*, **11**, 822–827.

Predy, R. & Malhotra, S.K. (1989) Reactive astrocytes in lesioned rat spinal cord: effect of neural transplants. *Brain Res. Bull.*, **22**, 81–87.

Ramon-Cueto, A., Plant, G.W., Avila, J. & Bunge, M.B. (1998) Long-distance axonal regeneration in the transected adult rat spinal cord is promoted by olfactory ensheathing glia transplants. *J. Neurosci.*, **18**, 3803–3815.

Reier, P.J., Houle, J.D., Jakeman, L., Winialski, D. & Tessler, A. (1988) Transplantation of fetal spinal cord tissue into acute and chronic hemisection and contusion lesions of the adult rat spinal cord. *Prog. Brain Res.*, **78**, 173–179.

Reynolds, B.A. & Weiss, S. (1992) Generation of neurons and astrocytes from isolated cells of the adult mammalian central nervous system. *Science*, **255**, 1707–1710.

Reynolds, B.A., Tetzlaff, W. & Weiss, S. (1992) A multipotent EGF-responsive striatal embryonic progenitor cell produces neurons and astrocytes. *J. Neurosci.*, **12**, 4565–4574.

Schreyer, D.J. & Skene, J.H. (1991) Fate of GAP-43 in ascending spinal axons of DRG neurons after peripheral nerve injury: delayed accumulation and correlation with regenerative potential. *J. Neurosci.*, **11**, 3738–3751.

Shah, K., Tang, Y., Breakefield, X. & Weissleder, R. (2003) Real-time imaging of TRAIL-induced apoptosis of glioma tumors in vivo. *Oncogene*, **22**, 6865–6872.

Shinmei, M., Miyauchi, S., Machida, A. & Miyazaki, K. (1992) Quantitation of chondroitin 4-sulfate and chondroitin 6-sulfate in pathologic joint fluid. *Arthritis Rheum.*, **35**, 1304–1308.

Silver, J. & Miller, J.H. (2004) Regeneration beyond the glial scar. *Nat. Rev. Neurosci.*, **5**, 146–156.

Snow, D.M., Lemmon, V., Carrino, D.A., Caplan, A.I. & Silver, J. (1990) Sulfated proteoglycans in astroglial barriers inhibit neurite outgrowth in vitro. *Exp. Neurol.*, **109**, 111–130.

Snow, D.M., Watanabe, M., Letourneau, P.C. & Silver, J. (1991) A chondroitin sulfate proteoglycan may influence the direction of retinal ganglion cell outgrowth. *Development*, **113**, 1473–1485.

Snow, D.M., Mullins, N. & Hynds, D.L. (2001) Nervous system-derived chondroitin sulfate proteoglycans regulate growth cone morphology and inhibit neurite outgrowth: a light, epifluorescence, and electron microscopy study. *Microsc. Res. Tech.*, **54**, 273–286.

Sweeney, T.J., Mailander, V., Tucker, A.A., Olomu, A.B., Zhang, W., Cao, Y., Negrin, R.S. & Contag, C.H. (1999) Visualizing the kinetics of tumor-cell clearance in living animals. *Proc. Natl Acad. Sci. U.S.A.*, **96**, 12 044–12 049.

Tang, X., Davies, J.E. & Davies, S.J. (2003) Changes in distribution, cell associations, and protein expression levels of NG2, neurocan, phosphacan, brevican, versican V2, and tenascin-C during acute to chronic maturation of spinal cord scar tissue. *J. Neurosci. Res.*, **71**, 427–444.

Teng, Y.D., Lavik, E.B., Qu, X., Park, K.I., Ourednik, J., Zurakowski, D., Langer, R. & Snyder, E.Y. (2002) Functional recovery following traumatic spinal cord injury mediated by a unique polymer scaffold seeded with neural stem cells. *Proc. Natl Acad. Sci. U.S.A.*, **99**, 3024–3029.

Tisay, K.T. & Key, B. (1999) The extracellular matrix modulates olfactory neurite outgrowth on ensheathing cells. *J. Neurosci.*, **19**, 9890–9899.

Ughrin, Y.M., Chen, Z.J. & Levine, J.M. (2003) Multiple regions of the NG2 proteoglycan inhibit neurite growth and induce growth cone collapse. *J. Neurosci.*, **23**, 175–186.

Watanabe, K., Nakamura, M., Iwanami, A., Fujita, Y., Kanemura, Y., Toyama, Y. & Okano, H. (2004) Comparison between fetal spinal-cord- and forebrain-derived neural stem/progenitor cells as a source of transplantation for spinal cord injury. *Dev. Neurosci.*, **26**, 275–287.

Yamagata, T., Saito, H., Habuchi, O. & Suzuki, S. (1968) Purification and properties of bacterial chondroitinases and chondrosulfatases. *J. Biol. Chem.*, **243**, 1523–1535.

Yick, L.W., Wu, W., So, K.F., Yip, H.K. & Shum, D.K. (2000) Chondroitinase ABC promotes axonal regeneration of Clarke's neurons after spinal cord injury. *Neuroreport*, **11**, 1063–1067.

Yick, L.W., Cheung, P.T., So, K.F. & Wu, W. (2003) Axonal regeneration of Clarke's neurons beyond the spinal cord injury scar after treatment with chondroitinase ABC. *Exp. Neurol.*, **182**, 160–168.

Yick, L.W., So, K.F., Cheung, P.T. & Wu, W.T. (2004) Lithium chloride reinforces the regeneration-promoting effect of chondroitinase ABC on rubrospinal neurons after spinal cord injury. *J. Neurotrauma*, **21**, 932–943.

Yu, X. & Bellamkonda, R.V. (2001) Dorsal root ganglia neurite extension is inhibited by mechanical and chondroitin sulfate-rich interfaces. *J. Neurosci. Res.*, **66**, 303–310.

Zuo, J., Neubauer, D., Dyess, K., Ferguson, T.A. & Muir, D. (1998) Degradation of chondroitin sulfate proteoglycan enhances the neurite-promoting potential of spinal cord tissue. *Exp. Neurol.*, **154**, 654–662.

Develop. Growth Differ. (2005) **47**, 501–510

Correlation between *Musashi-1* and *c-hairy-1* expression and cell proliferation activity in the developing intestine and stomach of both chicken and mouse

Rieko Asai,[1] Hideyuki Okano[2] and Sadao Yasugi[1,*]

[1]*Department of Biological Sciences, Graduate School of Science, Tokyo Metropolitan University, 1-1, Minamiosawa, Hachioji, Tokyo 192-0397, Japan and* [2]*Department of Physiology, Keio University School of Medicine, Shinjuku, Tokyo 160-8582, Japan*

Musashi-1 (Msi-1) is an RNA-binding protein that plays key roles in the maintenance of neural stem cell states and in their differentiation into neural cells. *Msi-1 has* also been proposed as a candidate marker gene of mammalian intestinal stem cells and their immediate lineages. In this study, we examined *Msi-1* expression in the small intestine and the stomach of both chicken and mouse during embryonic, fetal and postnatal development. In addition, we analyzed the expression of *c-hairy-1*, a chicken homologue of mouse *Hes1*, and assessed the proliferative activity of the cells expressing both of these factors. Significantly, during the development of these digestive organs in both species *Msi-1* expression showed dynamic changes, suggesting that it is important for digestive organ development, particularly for epithelial differentiation. Based on our observations of the expression patterns of *Msi-1* and *c-hairy-1* in the adult small intestine, we speculate that *Msi-1* is also a stem cell marker of the chicken small intestinal epithelium.

Key words: *c-hairy-1*, development, *Musashi-1*, small intestine, stem cells, stomach.

Introduction

Musashi-1 (*Msi-1*) is a gene encoding an RNA-binding protein, and was isolated as a mammalian homologue of *Drosophila Musashi*, which is required for the asymmetric cell division of sensory neural precursor cells in *Drosophila* (Nakamura *et al.* 1994). It was subsequently demonstrated that *Msi-1* is selectively expressed in neural progenitor cells, including stem cells, and has key roles in the maintenance of stem cell states and differentiation (Sakakibara & Okano 1997; Kaneko *et al.* 2000; Okano *et al.* 2002; Sakakibara *et al.* 2002). Thus, Msi-1 has been suggested to be a mammalian neural stem cell marker (Sakakibara *et al.* 1996).

Msi-1 is also expressed in the murine intestine (Sakakibara *et al.* 1996) and in the adult mouse small intestine where it is expressed in a few cells just above the Paneth cells in the crypts, where the predicted stem cell region exists, and in columnar cells located between Paneth cells at the crypt base. Moreover, the expression of *Msi-1* during the postnatal development of the murine small intestine is observed in the crypts (Kayahara *et al.* 2003). These observations therefore suggest that *Msi-1* is also a candidate marker of intestinal stem cells and their immediate descendant lineages (Booth & Potten 2000; Kayahara *et al.* 2003; Potten *et al.* 2003). In amphibians, *Msi-1* expression has also been shown to be upregulated by thyroid hormone in adult progenitor cells under the control of the connective tissue and plays an important role in their maintenance and/or active proliferation during gastrointestinal remodeling in this species (Ishizuya-Oka *et al.* 2003).

Recent studies have demonstrated that Hes1, a basic helix-loop-helix (bHLH) transcriptional factor regulated by Notch signaling (Jarriault *et al.* 1995), is essential for the self-renewal activity of neural stem cells and for repression of their commitment to neuronal lineages (Akazawa *et al.* 1992; Sasai *et al.* 1992). Additionally, Jensen *et al.* (2000) have reported that *Hes1*-deficient mice display excessive differentiation of multiple endocrine cell types in the developing small intestine, suggesting that Hes1 may be involved in the inhibition of small intestinal cell differentiation to endocrine cells, which is similar to its effects on neuronal differentiation. Kayahara *et al.* (2003)

*Author to whom all correspondence should be addressed.
Email: yasugi-sadao@c.metro-u.ac.jp
Received 14 April 2005; revised 11 August 2005; accepted 16 August 2005.

have recently shown that Hes1 co-localizes with Msi-1 in small intestinal crypts. It has also been suggested that Hes1 is involved in Paneth cell differentiation and in the maintenance of stem cells, and a working model has now been proposed whereby Musashi-1 activates Notch1 signaling through the translational repression of Numb, a Notch signal antagonist, which consequently leads to the expression of Hes1 (Suzuki *et al.* 2005). The chicken homologue of Hes1, *c-hairy-1*, is a member of the Hairy/Enhancer of split (H/E(spl)) family of bHLH transcriptional repressors, and is also both upregulated by, and mediates, Notch signaling (Takebayashi *et al.* 1994; Jarriault *et al.* 1995; Ohtsuka *et al.* 1999).

In contrast to the evidence that Msi-1 is a marker of adult intestinal stem cells, its function in the stomach has not yet been analyzed. In addition, its role, if any, in the morphogenesis and cytodifferentiation of digestive organs is not clear. In our current study, to further elucidate the functions of Msi-1, we examined its expression profile in the small intestine and stomach of both chicken and mouse during embryonic, fetal and postnatal development, and correlated these data with additional analyses of the expression of *c-hairy-1* and of cell proliferation activities.

Materials and methods

Animals and tissues

Embryos and hatched chickens of the white leghorn variety (*Gallus gallus domesticus*) were used in our experiments. Eggs were incubated at 38°C to reach each stage under study. For *in situ* hybridization and immunohistochemistry of tissue sections, the proventriculus (PV, glandular stomach) and the small intestine (SI) were collected from developing embryos on days 6, 9, 12 and 15 of incubation and from chickens 14 days after hatching. ICR mice were also examined in this study, and the SI and stomach (esophageal and glandular regions) were obtained from 13.5 (E13.5), 15.5 (E15.5) and 18.5 (E18.5) day fetuses, from postnatal 3 (P3), 10 (P10), or 21 (P21) day mice and from adult mice. Tissues were fixed with 4% paraformaldehyde, embedded in OCT compound (Tissue-Tek; Sakura Finetechnical, Tokyo, Japan) and sectioned at a thickness of 6 μm in a cryostat.

In situ *hybridization of frozen sections*

In situ hybridizations with digoxigenin-labeled RNA probes were performed on frozen sections as described previously (Ishii *et al.* 1997). An expressed sequence tag (EST) clone (clone ID: ChEST1015K21) containing an 840 bp cDNA fragment was used as the *Msi-1* probe. The *c-hairy-1* probe was generated from an expression plasmid provided by Dr O. Pourquié.

Immunohistochemistry

The sections were bleached with 3% H_2O_2 in methanol and heated in a microwave in 0.01 M citrate buffer (pH 6.0) for 7 min. The sections were then treated with blocking reagent-PBT (5% blocking reagent (Roche Diagnostics GmbH, Mannheim, Germany) in PBS plus 0.1% Tween-20), incubated with the primary antibodies anti-Msi-1 (1/500, biotin-conjugated; Kayahara *et al.* 2003), anti-PCNA (1/1000, Santa Cruz Biotechnology, Inc, Santa Cruz, CA, USA) or anti-Ki67 (YLEM, Rome, Italy) overnight at 4°C and washed three times in PBT. PCNA and Ki67 were used as proliferation markers. Sections incubated with the anti-Msi-1 antibody were immunostained using a Vectastain ABC kit (Vector Laboratories, Burlingame, CA, USA) according to the manufacturer's instructions. The sections treated with anti-PCNA antibody were incubated with Histofine Simple Stain Max-PO-Multi as a secondary antibody (Nichirei, Tokyo, Japan) for 60 min at room temperature. The sections treated with anti-Ki67 antibody were incubated with HRP-conjugated antirabbit IgG secondary antibody for 60 min at room temperature and the resulting signals were amplified using a TSA Biotin System (Perkin Elmer Life Sciences, Boston, MA, USA). After washing with PBT, color was developed with Histofine Simple Stain DAB (3,3′-diaminobenzidine) Solution (Nichirei, Tokyo, Japan) for 10 min. Sections were photographed with an Olympus BX-60 camera (Olympus, Tokyo, Japan) equipped with Nomarski optics.

Results

Expression of Msi-1 *during the development of the chicken small intestine*

During days 5–6 of incubation, the chicken SI is lined by an undifferentiated pseudostratified columnar epithelium (Romanoff 1960), which cannot be distinguished from the epithelia of other regions of the digestive tract. After day 6, however, each part of the digestive tract begins rapid morphological differentiation. In the SI at this stage, the epithelium forms a basic structure and active morphogenesis of the villi occurs (Coulombre & Coulombre 1958; Romanoff 1960; Hinni & Watterson 1963; Grey 1972). Moreover, the epithelial cells produce digestive enzymes such as sucrase (Matsushita 1983, 1985).